On Efficient Transmission Balancing Operation

Capturing the Normal State Frequency and Active Power Dynamics

MARTIN NILSSON

Licentiate Thesis
School of Electrical Engineering
KTH Royal Institute of Technology
Stockholm, Sweden 2018

TRITA-EE 2017:161
ISSN 1653-5146
ISBN 978-91-7729-595-2

KTH School of Electrical Engineering
SE-114 28 Stockholm
SWEDEN

Akademisk avhandling som med tillstånd av Kungl Tekniska högskolan framlägges till offentlig granskning för avläggande av licentiatexamen i elektriska energisystem onsdagen den 7 februari 2018 klockan 10:00 i L1, Drottning Kristinas väg 30, Kungl Tekniska högskolan, Stockholm.

Tryck: Universitetsservice US AB

Abstract

In an electric power system, there will always be an electric balance. Nevertheless, System Operators (SOs) often uses the term imbalance. Here, the term imbalance refers to the difference between trades and real-time measurements. This thesis defines the term imbalance and develops a framework helping SOs in finding better decisions controlling these imbalances.

Imbalances are controlled by many decisions made at various stages before real-time. A decision can be to increase the flexibility in production and consumption. However, this is not the only decision affecting real-time balancing operation. Other decisions are grid code requirements, such as ramp rates of HVDC and generation; balancing market structure, such as imbalance fees and trading period lengths; and the strategies used in the system-operational dispatch.

The purpose of this thesis is to create a new possibility for SO to find decisions improving the balancing operation. In order to find and compare decisions, the thesis develops a framework that evaluates many different decisions made at various stages before real-time. The framework consists of the following. First, it develops an intra-hour model using multi-bidding zone data from a historical time-period; able to capture the normal state frequency and active power dynamics. The model creates high-resolution data from low-resolution measurements using several data-processing methods. The uncertainty from the historical time-period is re-created using many sub-models with different input data, time-scales and activation times of reserves. Secondly, the framework validates the model and identifies system parameters based on simulated frequencies and frequency measurements in the normal state operation. Finally; new decisions' are modelled, tested, and evaluated on their impact on selected targets supporting corporate missions of the SOs.

The goal of the framework is that it should be able to find better decisions for balancing operation but also that it should be applicable for real and large power systems. To verify this, the framework is tested on a synchronous area containing 11 bidding zones in northern Europe. Results show that the framework can be validated and trusted.

Three new decisions, made at various stages before real time, have been modelled, tested and evaluated. The modelled decisions were (i) lower ramp rates for generation, (ii) increased capacities for automatic reserves, and (iii) a new strategy for the system-operational dispatch. One implication of applying the balancing evaluation framework on data from July 2015 is that all tested decisions improve several selected targets supporting the corporate missions of the SOs.

The conclusion is that the balancing framework is useful as a simulation tool in helping SOs in finding more efficient decisions for transmission system balancing operation.

Sammanfattning

I elektriska kraftsystem är det alltid elektrisk balans. Ändå används termen obalans. Med obalans avses i den här avhandlingen skillnaden mellan handel och faktiskt uppmätt produktion och konsumtion. Avhandlingen definierar denna obalans och skapar ett ramverk som kan hjälpa systemansvariga att finna bättre beslut för att kontrollera dessa obalanser.

Obalanser sker ständigt i kraftsystemen och om de inte skulle hanteras så skulle kraftsystemen kollapsa. Ett möjligt beslut är att öka flexibilitet i kraftsystemens produktions- och förbrukningskällor. Men detta är inte det enda beslutet som påverkar kraftbalansen i realtid. Andra beslut är bland annat ramphastigheter för produktion och HVDC-förbindelser mellan olika prisområden, designen och kapaciteterna av automatiska reserver, hur balansmarknaden är strukturerad, samt de strategier som används i de systemansvarigas kontrollrum.

Syftet med avhandlingen är att skapa nya möjligheter för de systemansvariga att kvantifiera olika besluts påverkan på balanseringen i normal drift. För att göra detta utvecklar avhandlingen ett ramverk som utvärderar många olika besluts påverkan på utvalda mätetal som stödjer de systemansvarigas mål och visioner. Först skapar ramverket en simulator som kan använda uppmätt data från en specifik tidsperiod. Simulatorn är uppbyggd av flera submodeller. En sub-modell transformerar uppmätt lågupplöst data till högupplöst data. Osäkerheten vid det historiska tillfället återskapas med hjälp av att flera sub-modeller använder olika indata, tidsskalor och att olika reserver har olika aktiveringstider. Modellen valideras och systemparametrar identifieras genom att jämföra högupplöst simulerad med uppmätt frekvens i normal drift. Den validerade modellen används som referensscenario när nya beslut modelleras, testas och utvärderas. Genom att koppla simulerade mätetal med de ansvariga systemoperatörernas mål och visioner kan ramverket utvärdera konsekvenserna av nya beslut tagna vid olika skeden före realtid.

Ramverket är utvecklat för att finna bättre sätt att balansera stora kraftsystem på. Det är också utvecklat för att var applicerbart på verkliga kraftsystem. Avhandlingen testar ramverket på det nordiska kraftsystemet som består av 11 prisområden. Tre nya beslut, tagna vid olika tidpunkter före realtid, modelleras, testas och utvärderas. De modellerade besluten är (i) nya ramphastigheter för produktionen, (ii) nya kapaciteter för automatiska reserver och (iii) en ny strategi i de systemansvarigas kontrollrum. Avhandlingen visar att de tre modellerade besluten förbättrar flera mätetal som stödjer de systemansvarigas mål och visioner.

Slutsatsen är att ramverket kan användas som ett simuleringsverktyg som kan hjälpa de systemansvariga att finna bättre beslut för en mer effektiv balansering av kraftsystemen.

Acknowledgements

I would like to express my gratitude to Svenska kraftnät for supporting and financing this project. It has been an interesting project where I found myself lucky to explore and search for the unknown in a topic I have had many years of work experience. It has been rewarding and fun having the possibility to strive for a goal for a long period of time. I would also like to thank the Department of Electric Power and Energy Systems at Kungliga Tekniska högskolan for your supervision.

I deeply thank my supervisor Professor Lennart Söder for his guidance in this project. You have often found time in your busy schedule and we have had several interesting discussions moving the project forward. I would also like to thank the IRES-research group at KTH. I think I have learned a lot from you both professionally and personally. I would also like to thank my co-supervisor Göran N Ericsson for making this possible. You understood already from the beginning that this approach could lead to an interesting trajectory in finding new solutions to an aging problem. Also thanks to Professor Mehrdad Ghandhari and Associate Professor Mikael Amelin for our collaborations and your help.

My deepest gratitude goes to my co-authors, colleagues and friends at KTH and Svenska kraftnät. Many thanks go to Egill, Ekatarina, Mahir, Anna and Dina for our lunches and good time together. Special thanks to Robert, Christer and Anders for your revision and contribution to this thesis. I also want to thank my managers Anna and Per for letting me do this and to my colleagues and friends at MS, MB and DB. Thanks to Madalena, Jonas, Julija, Lena, Mikael, Bo, Karolina, Maria, Bashir, Jesper, Marie, Pontus, Oskar, Linda, Tönn, Therese, Per-Olof, Johan, Viktor, Andreas, Jon and many others for all of your help. I would also like to thank Stefan, Taha, Omar, Poria, Viktor, Lars, Tin, Zhao, Francisco and Dimitrios for our time at KTH and at various conferences.

Finally, I would like to express my deepest gratitude to my closest friends and family for your support during this sometime challenging but learning journey. Thanks to my parents Göran and Birgitta and my siblings Maria, Marcus and Mikael for everything. Also, thanks to my friends at Myggöö GMK and Högbyligan for all the fun during these years. Also, two years ago my lovely son Casper was born. You and my lovely Caroline mean the world to me.

Martin Nilsson,
Sundbyberg, January 2018

Contents

List of Figures

List of Tables

List of Symbols

Indices	
$base.$	Measured subtracted by used reserves,
BC	Base Case,
$D(1,2,3)$	New decision 1, 2 or 3,
$forc.$	Forecasted,
fr	Fast Regulated production,
g	HVDC-lines, $g \in (1..G)$,
i	Integer, $i \in (1..I)$,
$iner.$	Inertial Response,
j	Integer, $j \in (1..J)$,
k	Operational dispatch 5min. data $(12m)$, $k \in (1..K)$,
m	Trading period data (hourly in NSA), $m \in (1..M)$,
$meas.$	Measured, or if not existing, planned or calculated,
n	Bidding zones, $n \in (1..N)$,
$plan$	Planned or forecasted,
PFC	Primary Frequency Control,
q	Iteration, $q \in (1..Q)$.
RSG	Re-Scheduled Generation,
s	1-second data $(3600m)$, $s \in (1..S)$.
$sim.$	Simulated,
SFC	Secondary Frequency Control,
sr	Slow Regulated production,
t	Real-time, $t \in (1..T)$,
$tot.$	Production, transmission subtracted by consumption,
$trad$	Traded,
w	Wind power production,
$\hat{}$	Transformed data.

Functions

$f(*)$	A data-processing method can be $K(*)$, $L(*)$ or $M(*)$,
$fabe(*)$	The software Frequency and Area Balancing Estimator (FABE)
$K(*)$	Data-processing method transforming frp,
$L(*)$	Data-processing method transforming srp, w and consumption,
$M(*)$	Data-processing method transforming HVDC-transmission.

Parameters

a_{CPS1}	Synchronous areas noise constant,
a_n	Linear regression offset parameter for area n,
AT	Activation time for TFC in k-resolution,
B	Frequency Bias Factor (K in Europe),
b_n	Linear regression slope parameter for area n,
ε	Total data processing error,
f_0	System nominal frequency, 50 Hz
FR	Fast Regulated (production), $s \in (0..1)$,
FRa	Fast Regulated ramp stop in minutes,
FRb	Fast Regulated ramp start in minutes,
γ	Step length, $\gamma \in Z^+$,
$H_{sys.}S_{sys.}$	System kinetic energy,
K_{RSG}	RSG confidence factor,
K_{TFC}	TFC confidence factor,
p_n	Proportional parameter used for SFC for area n,
$PFC_n^{cap.}$	PFC capacity for n areas (MW/Hz),

Time-series

$A_{n,m/k}$	Available data, can be P, C or T, for n areas of resolution m/k,
$C_{n,(m/s)}$	Consumption for n areas of resolution m/s,
$CPS1^{sim.}_{n,60s}$	Simulated CPS1 for n areas of 1-minute resolution
$D_{n,m}$	A variable time-series containing n areas of resolution m,
$e_{1,m}$	Synchronous areas measurement error,
$eACE^{sim.}_{n,s}$	Simulated estimated ACE for n areas of resolution s
f^{meas}_{s}	System frequency of resolution 5s
$f^{sim.}_{s}$	Simulated system frequency of resolution s
f_x	Control parameter for TFC activation's,
$\frac{df}{dt}$	System frequency deviation
$h_{n,m}$	Data processing error,
$L_{n,s}$	AC-tie line transmission for n bidding zones of resolution s
$P_{n,(m/s)}$	Production for n areas of resolution m/s,
$P^{sim.}_{TFCn,k}$	Simulated TFC activations of resolution s
$P^{sim.}_{RSGn,k}$	Simulated RSG activations of resolution s
$T_{(g/n),(m/s)}$	HVDC-transmission for n/g of resolution m/s
$V_{n,s}$	Variability for $P^{base}_{frp}, P^{meas.}_{(srp/w)}, C^{meas.}, T^{meas.}$,
$X_{n,m}$	Uncertainty for $P^{base}_{frp}, P^{meas.}_{(srp/w)}, C^{meas.}, T^{meas.}$,
$Y_{n,s}$	Imbalance for n areas of resolution s,
$Z_{n,m}$	Plan sub. trades for $P^{base}_{frp}, P^{meas.}_{(sr/w)}, C^{meas.}, T^{meas.}$,
Y_S	High-resolution imbalance in a synchronous area,
$x_{n,m}$	X-coordinate for area n and for sample m,
$y_{n,m}$	Y-coordinate for area n and for sample m.

List of Acronyms

ACE	Area Control Error,
AGC	Automatic Generation Control,
aFRR	automatic Frequency Restoration Reserves,
BC	Base Case,
FABE	Frequency and Area Balancing Estimator,
FCR-D	Frequency Containment Reserves 49.9-49.5Hz,
FCR-N	Frequency Containment Reserves ±0.1Hz,
FRP	Fast Regulated Production,
mFRR	manual Frequency Restoration Reserves,
NSA	Nordic Synchronous Area,
PFC	Primary Frequency Control,
RMSE	Root-Mean-Square Error
RSG	Re-Scheduled Generation,
SFC	Secondary Frequency Control,
SO	System Operator,
SRP	Slow Regulated Production,
TFC	Tertiary Frequency Control,
TS	Time Step.
vRES	variable Renewable Energy Sources.

Chapter 1

Introduction

This chapter presents an overview of the thesis. Section 1.1 summarizes the more extensive Chapter 2 which describes the background of the research area. Motivation, purpose and scope are presented in Section 1.2 and 1.3. A list of publications and the contributions are provided in Section 1.4 and 1.5. Finally, the outline of the remaining chapters is given in Section 1.6.

1.1 Background

Electrical power systems play an essential role in modern energy systems [3]. They have contributed to the enormous economic growth and created possibilities our societies could not have foreseen. Although the technology and ideas are old, our dependence on these systems has never been greater.

The world's first power system was built in 1881 to illuminate streets in England [4]. Electric power production was well understood; however, a significant difficulty with power systems is that electricity cannot be stored. Electrical power production has to meet electric power consumption continuously at all times [5]. Today, more than a century since the first power system was built; keeping continuous electrical power balance is still a great concern [6, 7].

In liberalised power markets, neutral organisations called System Operators (SOs) manage the power balance [8, 9]. These organisations are responsible for power system stability in real-time operation. Real-time operations are often divided into different security states [10]. Industry practice is to define an alert and a normal state using the N-1 criteria [5, 11, 12]. The normal state is a initial operating condition that is stable for all highly probable disturbances. Power system stability is defined by [5]:

* *Power system stability is the ability of an electric power system, for a given initial operating condition, to regain a state of operating equilibrium after being subjected to a physical disturbance, with most system variables bounded so that practically the entire system remains intact.*

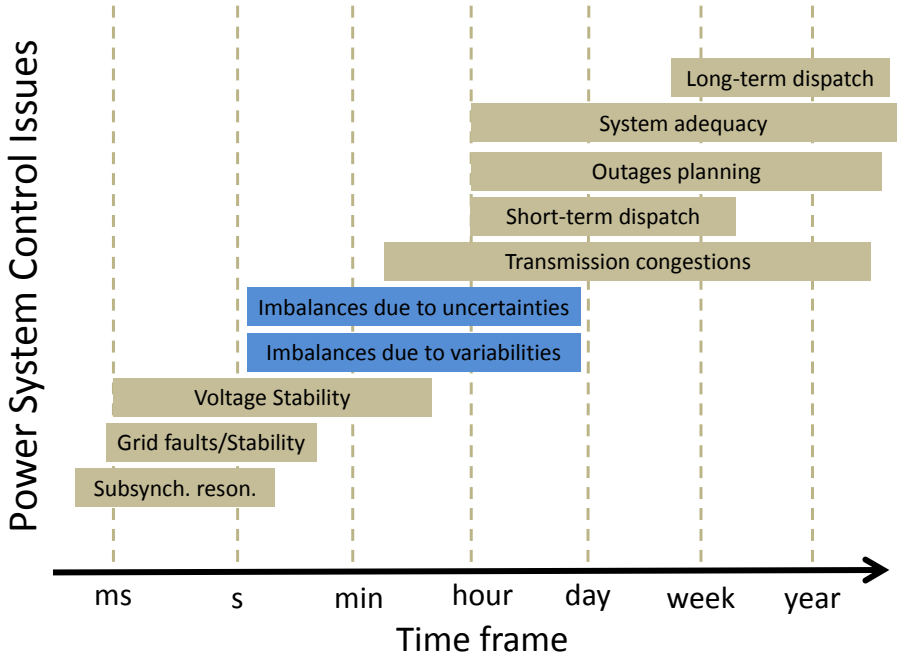

Figure 1.1: Power-system-control issues occurs in many different time frames. Highlighted in blue are the control issues addressed in this thesis.

To be stable power systems are designed to handle many different control issues [13]. Figure 1.1 shows different control issues that occur in various time frames. This thesis addresses the normal state imbalance control issue due to variabilities and uncertainties.

In electric power systems, there will always be an electrical balance. However, System Operators (SOs) often use the term imbalance. Historically, the cause of these imbalances, in the normal state operation, was assumed to originate from consumption [14, 15]. The conventional generation can adhere to their traded production plans, and imbalances typically were not created from this origin. However, due to the extensive accommodation of variable Renewable Energy Sources (vRES) [6], increased HVDC-capacities [16, 17] and the deregulation of electricity markets [18]; imbalances can, in a considerable larger extent, originate from production and coordination between production and HVDC-transmission. Therefore, many power systems worldwide have detected increased imbalances [18, 19], and with increased accommodations of vRES, more imbalances are foreseen [20].

In electric power system terminology, the term imbalance can have several different meanings. The term imbalance (Y(t)) is here referred to as the difference

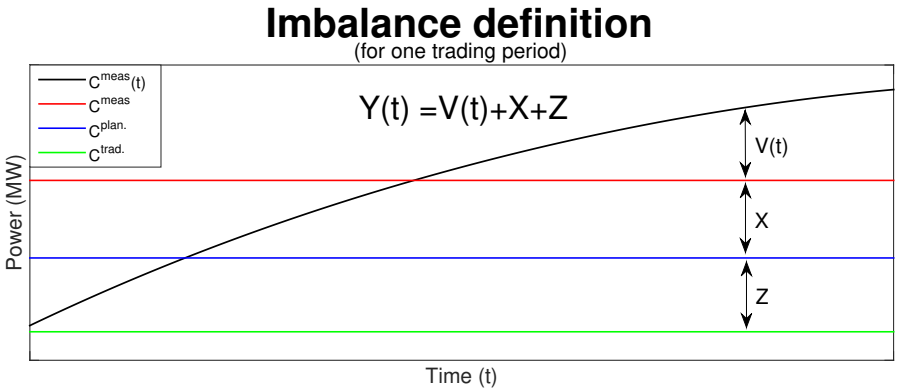

Figure 1.2: Imbalance definition. The term imbalance (Y) is divided into variability (V), uncertainty (X) and difference between forecasts and trades (Z) for one trading period. The illustration is for consumption (C).

between traded and real-time (t) measurements within a trading period (e.g. one hour in the Nordic power system). This thesis divides the imbalance into three components. Figure 1.2 illustrates the imbalance definition for one trading period and these three components. The Figure illustrate the imbalance for consumption (C); however, the illustration is valid for all used origins in this thesis.

First component is called variability (V). The variability ($V(t)$) is here defined in high-resolution as the difference between real-time measurements and the average trading-period measurements. Thus, the integration over a trading-period is zero.

The second component is called uncertainty (X). The uncertainty (X) is here defined for a trading period as the difference between average trading-period measurements and the latest trading-period forecasts, i.e. constant value for each trading period.

The third component is called the difference between forecasted and traded (Z). This component (Z) is here defined for a trading period as the difference between the latest trading-period forecasts and the trading-period trades, i.e. constant value for each trading period.

1.2 Motivation

Today, imbalances are in a larger extent originated from other sources than consumption [6, 16, 18, 17, 19]. Therefore, many power systems worldwide have detected increased imbalances [18, 19], and with increased accommodations of vRES,

more imbalances are foreseen [20].

Integration of vRES has been intensively studied including its impact on system adequacy, economic dispatch, transmission congestions and various stability issues [21]. However, in the range of its impact on imbalances in the normal state operation within and between trading periods more studies are needed. A technical target for the normal state operations is to maintain the system inside predefined security boundaries [22, 23]. An economical target is to full-fill the technical target in an economical way [24, 25].

Many different decisions made at various stages before real-time handle power system imbalances in the normal state operations [18, 19]. One decision is to increase the flexibility in generation [26] and consumption [7]. However, neither is it the only decision affecting the normal state balancing operation nor it seems to be the most efficient [19]. Other decisions affecting the normal state balancing operation are strategies for System Operational dispatch, various grid code requirements and the balancing market structure. Figure 1.3 illustrates these different decision made at various stages before real-time. The various stages can be explained as follows.

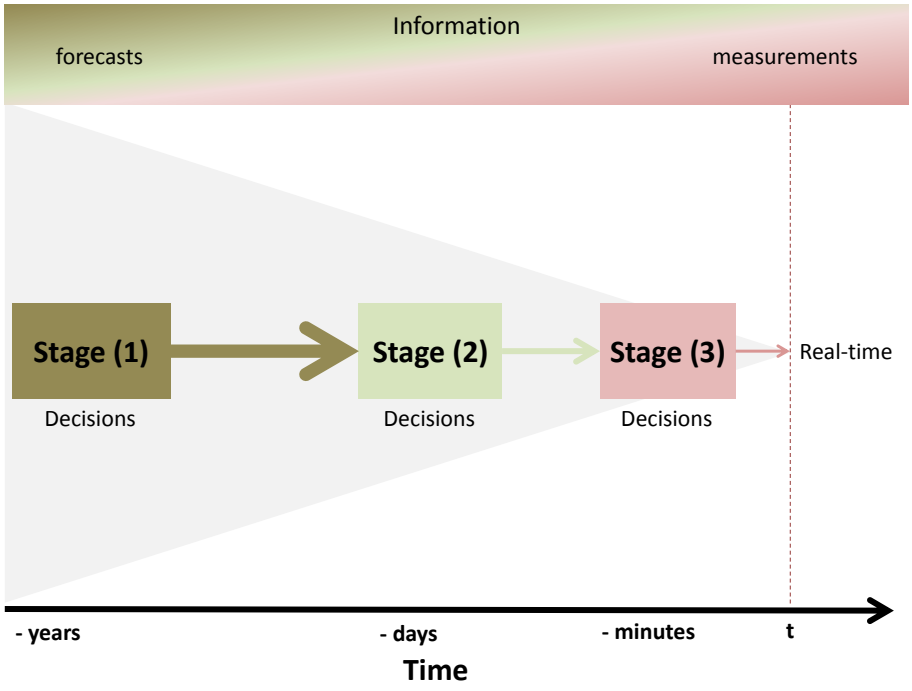

Figure 1.3: Different transmission-system balancing decisions made at various stages before real-time.

Stage (1) Power system operational design. Years before real-time, decisions on power system design are made. Decisions made at this stage can be establishing grid-code requirements and balancing market structure. Grid code requirements can be ramp-rates for generation and HVDC-transmission between different balancing areas [16, 27]. It can also be automatic and manual reserve capacities, activation time and other design conditions. Balancing-market structure can be imbalance-settlement fees and the procurement process of different system services. These decisions can have an impact on decisions made at Stage (2) and Stage (3).

Stage (2) Planning operations. Days before real-time, different decisions of operational planning are made. Decisions made at this stage can be unit commitment, short-term outage planning, trade-capacities between bidding zones and the procurement of automatic reserves. These decisions can have an impact on decisions made at Stage (3).

Stage (3) Operational dispatch. Minutes before real-time, decisions of operational dispatch are made [28]. It is most often re-scheduling of production or consumption, but it can also be handling of HVDC-transmissions loops [29] or AC-loops using phase-shifting transformers.

The present and future penetration of vRES has increased the need to quantify how these different decisions affect the balancing operation [20, 30]. This creates large needs for new models, methods and frameworks; enabling new types of transmission system flexible adequacy studies; able to capture the normal state frequency and active power dynamics. These new models, methods and frameworks can help SOs in finding more efficient balancing operation. However, to the authors' best knowledge: models, methods and frameworks that evaluates many different decisions impact on SOs missions does not exist.

1.3 Purpose and scope

The purpose of this thesis is to create a new possibility for SO to find decisions improving the balancing operation. In order to find and compare decisions; this thesis first step is to develop a framework for the normal state balancing operation. The framework needs to be able to quantify many different decisions impact on selected targets supporting corporate missions of the SOs. These different decisions may have been made at various stages before real-time and possibly having an impact on one another.

The scope of this thesis is to create and test a framework that can evaluate many different decisions impact on selected targets supporting the SOs missions. In order to apply and test the framework on real power systems; this thesis develops an intra-hour model that can use available data from a historical time-period.

The intra-hour model is called Frequency and Area Balancing Estimator (FABE). One important reason when developing the idea of the work leading to this thesis was that, in many power systems, independently measured time-series of frequency response and low-resolution production, consumption and HVDC-transmission are publicly available. These independent measurements are used to validate FABE and identify unknown system parameters for a simulations time-period (T).

The intra-hour model (FABE), illustrated in Figure 1.4, uses available data from a historical time-period (T). The available data is bidding-zone data, such as measurements, plans and forecasts. One advantage using data from a historical time-period is that it can be used to re-create the variability and uncertainty. Another advantage is that it makes it possible to validate the model set-up against independent frequency measurements. Also, the validated set-up can be used as a reference scenario performing studies comparing the impact of new decisions.

FABE consists of several Sub-Models with multiple time-scales. Two different time-scales are used. The first time-scale is the high-resolution time-scale (s) and the second time-scale is the five minute (k) time-scale.

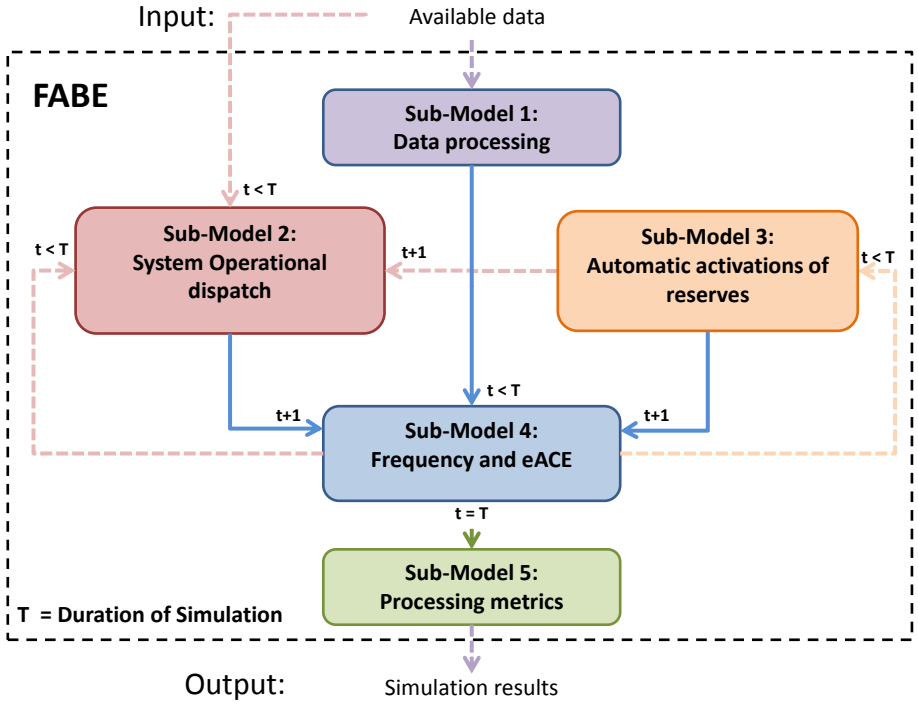

Figure 1.4: Frequency and Area Balancing Estimator (FABE). FABE is used in a framework to evaluate many different decisions made at various stages before real-time. The model is divided into five Sub-Models.

Table 1.1: Testing different decisions made at various stages shown in Figure 1.3 by one or two changes in Sub-Models shown in Figure 1.4.

	Stages: (Figure 1.3)			Sub-Models: (Figure 1.4)				
Decisions	(1)	(2)	(3)	1	2	3	4	5
Ramp rates for HVDC & gen.	X			X				
Automatic reserves: design and capacities	X	X				X		
Trading period length	X			X				
System-operational-dispatch strategies			X		X			
Power system generation mix	X			X				
Forecasts of vRES & consumption		X	X		X			
Activation time of SOs dispatch	X				X			
System Operators targets & missions	X							X

FABE creates a possibility for SOs to test new decisions made at various stages before real-time. Decisions made at various stages before real-time can be tested by changing the set-up in one or two Sub-Models in FABE. Table 1.1 compiles needed changes when testing new decisions.

FABE and its Sub-Models are explained in the following way:

FABE input: Available data.
Available input data is multi-bidding-zone hourly measurements and five-minute schedules and forecasts from one time-period (T). The time-period (T) can be an hour to months or even years; however, in this thesis, the time-period of one month is tested.

Data is here referred to as low- and high-resolution data. Low-resolution data is hourly measurements (resolution m) and five-minute schedules and forecasts (resolution k) of production, consumption and HVDC-transmission. High-resolution data is five-second (resolution 5s) and one-second (resolution s) data.

Sub-Model 1 Data processing.

Input: data is comparatively low-resolution data, such as hourly measurements (m) for each bidding zone (n) and/or HVDC-transmission line (g) for a specific time-period (T).

Output: data is high-resolution data (s) for each bidding zone (n) such as production, consumption, HVDC-transmission and a re-created imbalance time-series.

Low-to-high-resolution transformation of data time-series of production, consumption and HVDC-transmission are performed using various data-processing methods. These transformations are performed on the data time-series for the whole time-period (T) at once. These methods create the variability (V), see Figure 1.2, within each trading period. Also, the Sub-Model re-creates an imbalance time-series subtracting the historical uncertainty and the difference between forecasts and trades (X+Z) for each trading period.

Testable decisions at this Sub-Model are compiled in Table 1.1. It can be different grid code requirements such as ramp-rates of generation and HVDC-transmission and/or different trading period lengths.

Sub-Model 2 System-operational dispatch.

Input: data is available data such as scheduled and forecasted production, consumption and HVDC-transmission for each bidding zone. Input data data are also (from Sub-Model 4): simulated frequency response and calculated eACE (see Section 3.5 for details); and (from Sub-Model 3): activated automatic reserves.

Output: data is system-operational-dispatch decisions.

System-operational-dispatch decisions are made some minutes before real-time. These decisions are based on modelled routines and input data.

Testable decisions at this Sub-Model are compiled in Table 1.1. It can be decisions of new dispatch strategies as-well as decisions leading to forecast improvements of vRES and consumption and/or various activation times for manual reserves.

Sub-Model 3 Activation of automatic reserves.

Input: data is (from Sub-Model 4) simulated frequency response and eACE.

Output: data is activated automatic reserves.

In all power systems, automatic reserves exist with the aim to keep the frequency within its normal state security boundaries and sometimes restoring ACE for each balancing area[5].

Testable decisions at this Sub-Model are compiled in Table 1.1. It can be new designs, capacities and/or new types of automatic reserves.

Sub-Model 4 Frequency and eACE.

Input: data for each bidding zone (n) is (from Sub-Model 4): high-resolution imbalance, production, consumption and HVDC-transmission; and (from Sub-Model 3): activated automatic reserves; and (from Sub-Model 2): activated system-operational dispatches.

Output: data is frequency and eACE.

Input data from several Sub-Models are used to simulate frequency and eACE.

No testable decisions are possible at this Sub-Model. This Sub-Model only simulates frequency and eACE.

Sub-Model 5 Processing metrics.

Input: data is time-series of simulation result for a tested time-period (T) from all Sub-Models. It can be simulated frequency response, eACE, activated automatic reserves and activated system-operational dispatches.

Output: data is balancing metrics such as frequency quality, the standard deviation of eACE and average used reserves for the simulated time-period (T).

A decision scenario's simulation results for a time-period (T) can be evaluated depending on its impact on different balancing metrics.

Testable decisions at this Sub-Model are compiled in Table 1.1. It can be the interpretation of the System Operators missions creating different balancing metrics.

FABE output: Simulation results.
Simulation results are data from all Sub-Models. It can be targets and metrics, simulated frequency response, eACE and/or activated manual and automatic reserves among others.

The Balancing Evaluation Framework (BEF), shown in Figure 1.5, creates and uses the intra-hour model (FABE) to quantify and evaluate many different decisions impact on balancing operation. The framework is illustrated in Figure 1.5 and can be explained as follows:

1. The framework creates the intra-hour model (FABE).
2. The framework uses FABE to identify system parameters using data from a historical time-period and various statistical tools.

3. With identified system parameters from a historical time-period, the framework validates FABE using historical data from another time-period using various validation methods.

4. A new decision can be modelled using FABE with unchanged validated system parameters except for one or two changes in the model - needed to test investigated new decision.

5. Simulation results for a new decision can be evaluated and compared against the validated reference scenario based on selected targets supporting the corporate missions of the SOs.

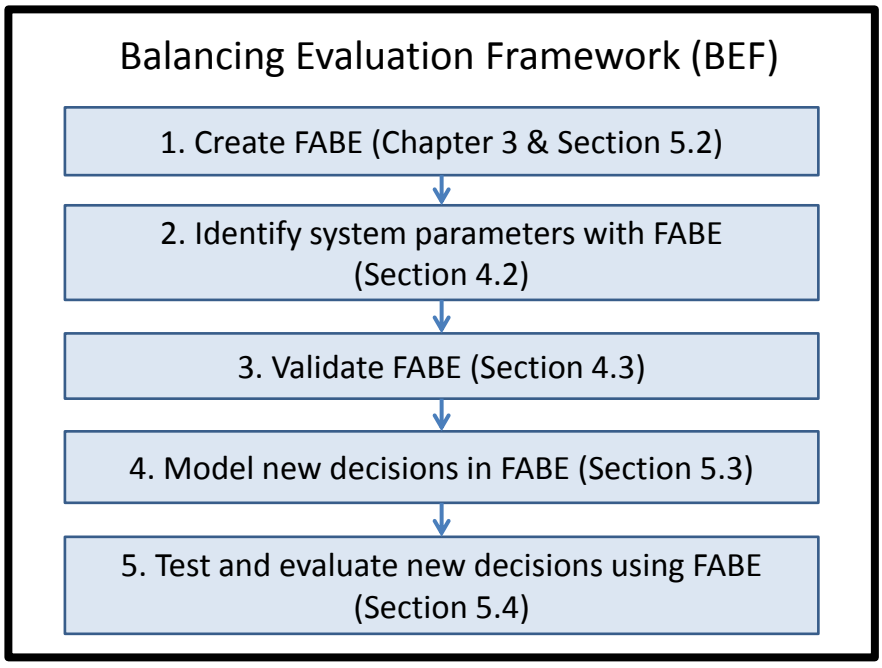

Figure 1.5: Balancing Evaluation Framework (BEF) that evaluates different decisions impact on selected targets supporting the corporate missions of the SOs.

1.4 List of publications

The following papers have been published (so far) during the PhD studies.

Papers presented in journals:

[J1] M. Nilsson, L. Söder, and G. N. Ericsson, "Balancing strategies evaluation framework using available multi-area data,"*IEEE Transactions on Power Systems*, vol. PP, no. 99, pp. 1–1, 2017.

Peer-reviewed conference papers:

[C1] M. Nilsson, L. Söder, and Z. Yuan, "Estimation of power system frequency response based on measured & simulated frequencies," in 2016 *IEEE Power and Energy Society General Meeting (PESGM)*, July 2016, pp. 1–5.

[C2] M. Nilsson, L. Söder, R. Eriksson, M. Ghandhari, and G. N. Ericsson, "Designing new proactive control-room strategies to decrease the need for automatic reserves," in 2017 *IEEE International Conference on Innovative Smart Grid Technologies (ISGT)*, September 2017, pp. 1–6.

[C3] M. Nilsson, L. Söder, and G. N. Ericsson, "Evaluation of different strategies for frequency quality control," in 2016 *Biennial International Conference on Power and Energy Systems: Towards Sustainable Energy (PESTSE)*, January 2016, pp. 1–6.

Division of the work between the authors

Publications J1, C1, C2, and C3, M. Nilsson drew the outline, carried out the work and wrote these publications under the supervision of the co-authors except for [C1], where Z. Yuan wrote one subsection.

1.5 Research contributions

This licentiate thesis' major contributions are the Balancing Evaluation Framework (BEF) and the intra-hour model (FABE). While developing these major contributions the thesis includes several minor contributions. Table 1.2 compiles the contributions, publications and chapters.

This thesis contribution is as follows:

Major Contribution 1 Balancing Evaluation Framework (BEF).
This thesis develops a balancing evaluation framework that evaluates many different decisions impact on targets supporting SOs missions. The framework is applicable to real and large power systems. The framework (BEF) has been published in publication [J1], but essential parts have also been published in [C1], [C2] and [C3].

Table 1.2: Contributions in publications and chapters of the thesis.

Contribution	**Publication**				**Chapters**			
	J1	C1	C2	C3	2	3	4	5
Major Contribution 1	X	X	X	X	X	X	X	X
Major Contribution 2	X	X	X	X		X		X
Minor Contribution 1	X	X		X		X		
Minor Contribution 2	X	X		X			X	
Minor Contribution 3	X						X	
Minor Contribution 4			X			X		
Minor Contribution 5	X					X		
Minor Contribution 6	X				X			
Minor Contribution 7	X							X
Minor Contribution 8	X		X					X

Major Contribution 2 Frequency and Area Balancing Estimator (FABE).
This thesis develops an intra-hour model called FABE. FABE can be used in the framework BEF but it can also be used for other purposes. FABE simulates frequency and eACE using several Sub-Models with multiple time-scales. The intra-hour model (FABE) has been published in publication [J1], but essential parts of the intra-hour model have also been published in [C1], [C2] and [C3].

Minor Contribution 1 Re-creating historical imbalance time-series.
To re-create a historical imbalance time-series one needs to transform data from a historical time-period. Section 3.2 presents the creation of a high-resolution imbalance time-series. These methods have been published in publication [J1], [C1] and [C3].

Minor Contribution 2 System-parameter identification.
One approach for intra-hour model system-parameter identification is to use high-resolution frequency response measurements from one or several disturbances [31, 32]. This approach may be accurate enough for models addressing control issues that occur during disturbances however, when investigating control issues that occur in the normal state operation this approach may give inaccurate system parameters. This thesis approach instead is to identify system parameters during the normal state operations based on high-resolution frequency measurements and simulated

frequencies. Various statistical tools are used in several different methods. These methods have been published in publication [J1], [C1] and [C3].

Minor Contribution 3 Model validation.
One approach to validate an intra-hour model is to use high-resolution frequency measurements from another or several independent disturbances [31, 32]. This thesis approach is to validate the intra-hour model based on frequency measurements during the normal state operations using other data time-series from the same investigated time-period than the data used for system parameter identification. Results are analysed using various validation methods. Publication [J1] has published these methods.

Minor Contribution 4 System-operational-dispatch modelling.
System-operational dispatch has to be modelled to capture the dynamics in the normal state operation. This thesis approach is to use simple and understandable algorithms modelling two separated control-room processes. Publication [C2] has published these algorithms.

Minor Contribution 5 ACE calculation without a network.
ACE calculations are by definition in need of a network. Here we estimate each bidding zones ACE using measurements and schedules from a historical time-period. An advantage using this approach is that no network model is needed to estimate ACE. Publication [J1] has published the model and the equations.

Minor Contribution 6 Defining imbalance in the normal state operation.
The term imbalance can be defined differently in various time frames. Imbalance in the normal state operation can be defined as the difference between trades and real-time measurements. This thesis divides the imbalance into three different components. One component is variability, another is uncertainty, and the third component is a difference between forecasts and trades. Publication [J1] has published the imbalance definition used in this thesis.

Minor Contribution 7 Identifying targets supporting the corporate missions of the SOs.
To find a good decision, one first needs to define what a good decision is. For a SO, a good decision is a decision supporting their missions. This thesis has identified targets supporting the corporate missions of the ENTSO-E. Publication [J1] has published these targets.

Minor Contribution 8 Model, test and evaluate new decisions.
This thesis develops a Balancing Evaluation Framework (BEF). The framework has been tested evaluating new decisions modelled in FABE. These decisions have been modelled and analysed in publication [J1] and [C2].

1.6 Thesis outline

The remaining chapters of this thesis are organized as follows.

Chapter 2 provides the background to the topic. Different power system control issues, various intra-hour analysing tools and general knowledge to power system operational states are presented. Finally, it presents the imbalance definition, used in this thesis, consisting of three components.

Chapter 3 builds the intra-hour model (FABE) using available historical multi-bidding-zone data. The concept of available data is presented, and different methods are transforming low-resolution data to create a high-resolution imbalance time-series. Modelling system-operational dispatch and automatic reserves are expressed in algorithms and equations. Finally, it presents the frequency and estimated ACE (eACE) derivation.

Chapter 4 validates the model and identifies system parameters from a historical time-period. It ends by presenting the validated reference scenario used when evaluating new decisions.

Chapter 5 applies the framework that evaluates different decisions impact on balancing operation. It identifies targets supporting the corporate missions of the SOs to be processed to metrics in Sub-Model 5. Modelling new decisions are performed and tested on a real power system. Finally, results are evaluated, and recommendations are presented.

Chapter 6 concludes the thesis and provides possible directions for future research.

Chapter 2

Background

This chapter presents the background to the topic. Section 2.3 and 2.5 are based on [J1]. It introduces different power system control issues in Section 2.2 and some intra-hour analysing tools in Section 2.3. General used power system operational states are presented in Section 2.4. Finally, the imbalance definition used in this thesis is presented in Section 2.5.

2.1 Introduction

Electrical power systems play an important role in modern energy systems. Large power systems use a high-voltage transmission grid to transfer power between areas. In liberalised markets, these high-voltage transmission grids are operated by neutral organisations. These organisations are called Transmission System Operators (TSOs) in Europe. In the United States, similar organisations are called Independent System Operators (ISOs) and Regional Transmission Organizations (RTOs). Safety and reliability are critical issues for these organisations. Since operational failures can lead to large economic damages, a goal is to have a secure and reliable power system.

This chapter presents some important background to this thesis. Section 2.2 presents power system control issues that occur in different time-frames. The section emphasises that all these control issues have to be handled to have a secure power system operation. Several different analysing tools are used to analyse these control issues depending on their time-frame. The analysed control issue in this thesis is the imbalance control issue occurring in the time frame from seconds to days. Section 2.3 presents several existing intra-hour analysing tools used to analyse the imbalance control issue that this thesis address. Section 2.4 presents power system operational states. This thesis analyses imbalances in the normal state operation. Finally, Section 2.5 presents the imbalance definition developed and used in this thesis to clarify the meaning by the term imbalance.

2.2 Power system control issues

A secure and reliable transmission system needs to control many different power system phenomena [13]. Figure 2.1 shows different power system control issues and in what time-frame they occur. To perform analyses on various control issues different types of analysing tools are available. Details of the model and valid assumptions depend on the analysed control issue and the analysed time-frame. This thesis divides analysing tools into three different types (Type A, B, C) depending on the time frame it addresses. Figure 2.1 illustrate the connection of time-frames, control issues and type of analysing tools. The types of analysing tools are explained as follows.

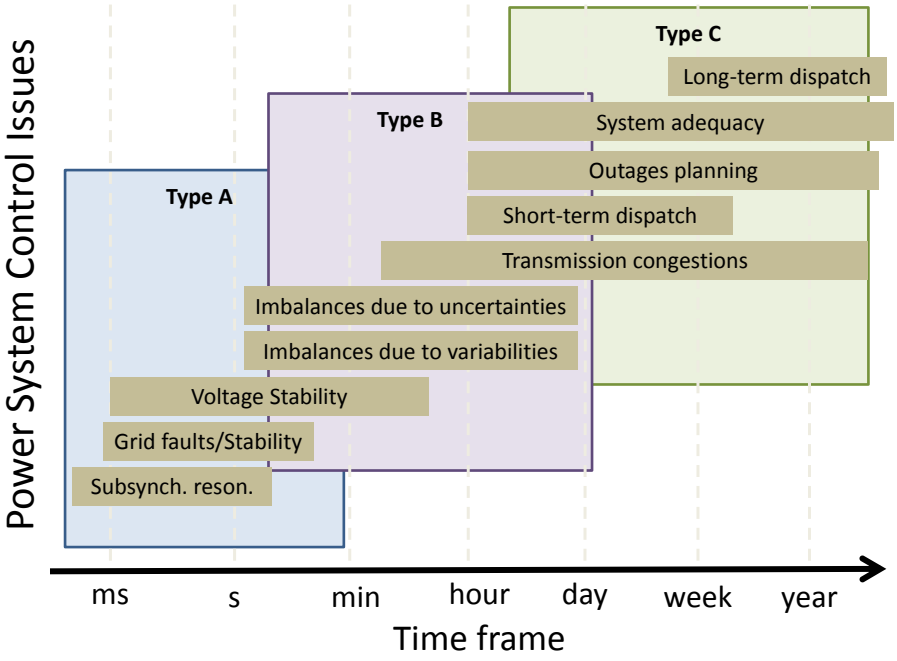

Figure 2.1: Power system control issues in different time frames.

Type A Models with enough details to capture voltage, frequency and rotor angel steady state and dynamic behaviours are used. Analysed time-frame is often from milliseconds to several seconds. Analysed control issues can be contingency analyses for voltage, frequency and rotor angle stability. These studies can be performed to define the ranges of various system variables for the

operational security states.

Type B Enough detailed models are needed to capture system frequency, active power and voltage dynamic behaviours within and for several trading periods. Grid-models can be used depending on analysed control issue [33, 34, 35]. Analysed control issues can be imbalances due to variability and uncertainty within and for several trading periods. Schedules are needed in an operational-dispatch Sub-Model to capture imbalances due to uncertainty. Often, studies addressing these control issues uses hybrid approaches with both measurements from a historical time-period and results from an economic-dispatch [33, 34, 35].

Type C Models with enough details are used to capture the economic dispatch behaviours within and for several days, weeks and years. Used details of grid-models can vary between studies and tools. Analyzed control issues can be the unit commitment, long- and short-term dispatch, outage planning, and power system expansion planning.

2.3 Intra-hour analysing tools

Intra-hour analysing tools address power system control issues described as "Type B" in Section 2.2, illustrated in Figure 2.1. Different decisions made at various stages before real-time affect the normal state dynamics and the imbalance control issue. Decisions can be network requirements, market design and/or strategies used in the system-operational dispatch. One approach to analyse the imbalance control issue is by using intra-hour analysing tools.

The intra-hour model developed in this thesis uses available multi-area data. It is called Frequency and Area Balancing Estimator (FABE) and analyses the imbalance control issue, capturing frequency and active power dynamics. FABE, similar to FESTIV [33], KERMIT [34], and ESIOS [35], fills the gap between analysing tools addressing the time frame from seconds to days within and between trading-periods. All these tools have several similarities and uses multiple time-scales within different Sub-Models. However, Table 2.1 compiles some differences between the previous mentioned intra-hour analysing tools.

FESTIV includes Sub-Models of security-constrained unit-commitment, security-constrained economic dispatch, and automatic generation control. The software has been used to quantify the impact of different market design and different system-operational-dispatch strategies impact on balancing operation [36].

KERMIT includes Sub-Models of security-constrained economic dispatch, automatic generation control and frequency deviations. Historical measured and scheduled data are processed and used as input in various Sub-Models. The software program has been used to perform reserve adequacy studies in systems with substantial accommodation of vRES [26].

Table 2.1: Some differences between intra-hour analysing tools

	FESTIV	KERMIT	ESIOS	FABE
Using data from a historical time-period?	no	consumption, variable Renewable Energy Sources	consumption, variable Renewable Energy Sources	consumption, production, HVDC, variable Renewable Energy Sources
Resolution	6 second	1 second	10 second	1 second
Areas	multi	single	single	multi
Validation	detailed model	contingencies-$\frac{df}{dt}$, -f	ACE, AGC, CPS2	the normal-state frequency (f)
Output	ACE, CPS2, prod. costs	CPS1, CPS2, f	ACE, AGC, CPS2	ACE, CPS1, f

ESIOS includes Sub-Models of Operational dispatch and automatic generation control. Historical measured and scheduled data are processed and used as input in various Sub-Models. The software program has been used to perform large-scale photo-voltaic integration studies on balancing operation [37].

FABE, similar to FESTIV, KERMIT and ESIOS, uses several Sub-Models with various time-scales. However, these programs, in contrast to FABE, have some drawbacks performing intra-hour analyses quantifying the impact of many different decisions on the normal state balancing operation. One drawback is that production measurements from a historical time-period cannot be used as input data. By using production measurements FABE can identify system parameters and be verified based on independent measurements in the normal state operation.

2.4 Power system operational states

Power system operation requires a balance between security and economy when delivering electricity from power production sources to satisfy the consumption [10]. From a technical viewpoint power system operation achieves this most efficiently depending on characteristics of the production, the high-voltage transmission grid, and the consumption. The approach to full-fill this is often to use different operational routines depending on the real-time system operational state.

Operational states are often defined using power system analysing tools performing various stability analyses in time frames from milliseconds to minutes. These system-state classifications help SOs managing their power systems. The normal state pre-classified ranges of system variables are here referred to as the system variables security range. Figure 2.2 shows commonly used system states [10].

Commonly used transmission system operational states can be explained as follows.

Normal is a state with all variables within their security ranges. In this secure state, highly probable contingencies can occur without

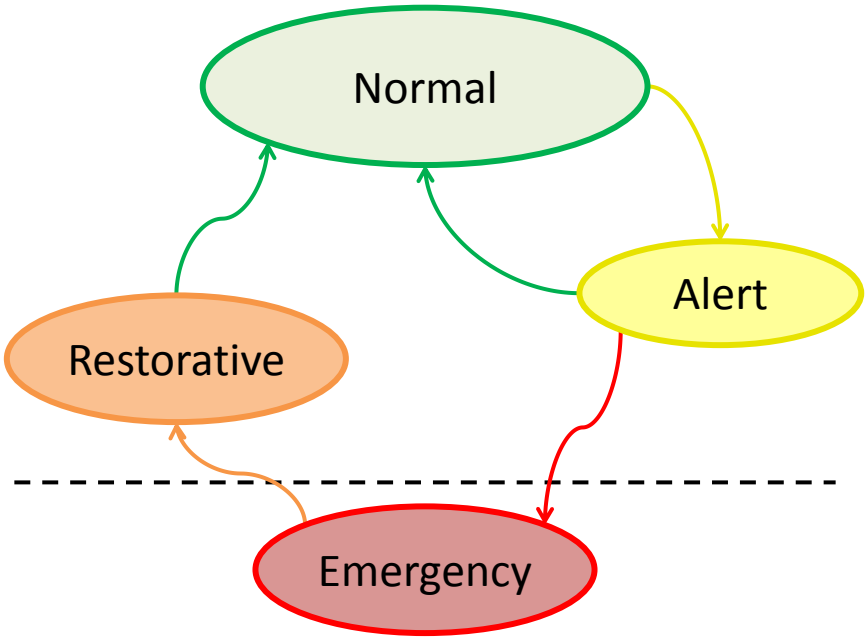

Figure 2.2: Transmission system states.

leading to the emergency state [38]. The technical objective in this state is to keep the system variables inside their predefined security ranges. Another objective is to full-fill the technical objective economically. These predefined ranges for system variables can be obtained performing analyses using the N-1 criteria. However, research has been performed on more probabilistic based secure management strategies [39].

Alert is a stable state where one or several system variables are outside their normal state security ranges. Even though the state is stable, if a highly probable contingency would occur the system may move to the emergency state [38].

Emergency is a *sate* that reflects a collapse of the power system leading to regional or in worst case system blackouts [10].

Restorative is a state energizing the system and reconnecting/re-synchronizing different parts of the system [38].

2.5 Defining the term imbalance

In electric power system terminology, the term imbalance can have several different meanings. This thesis defines the term imbalance in the time-frame from seconds to days as the difference between real-time measurement and trades. The term imbalance $Y(t)$ is defined as the difference between real-time measurement and traded. It is divided into variability $V_m(t)$, uncertainty X_m and difference between forecasts and trades Z_m for each trading period and defined be (2.1).

$$Y(t) = V_m(t) + X_m + Z_m \qquad \forall m \tag{2.1}$$

The defined imbalance can be used for production, consumption and/or HVDC-transmission. It can be used for a power system, a synchronous area, and/or several bidding zones. Figure 2.3 illustrates the imbalance definition developed in this thesis for two trading periods (m and m+1) and the three components the imbalance consists of. The Figure illustrates imbalances for consumption (C); however, the imbalance definition is valid for all sources and trading periods.

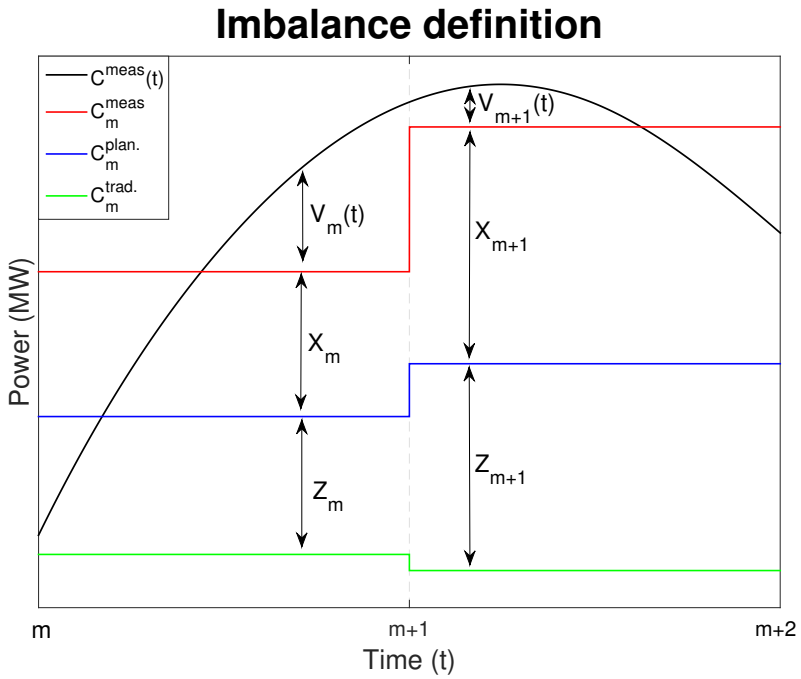

Figure 2.3: Imbalance definition. The term imbalance $Y(t)$ is the difference between real-time measurements and trades. It is divided into variability $V_m(t)$, uncertainty X_m and difference between forecasts and trades Z_m.

The imbalance can also be explained as follows.

First component is called variability (V). The variability ($V_m(t)$) is here defined for a trading period (m) in high-resolution (resolution s) as the difference between real-time measurements and the average trading-period measurements (resolution m). Thus, the integration over a trading-period is zero, ($\int_{m-1}^{m} V_m(t)\,\mathrm{d}t = 0$).

The second component is called uncertainty (X). The uncertainty (X_m) is in this thesis defined for a trading period (m) as the difference between average trading-period measurements and the latest trading-period forecasts, i.e. constant value for each trading period.

The third component is called the difference between forecasts and trades (Z). This component (Z_m) is in this thesis defined for a trading period (m) as the difference between the latest trading-period forecasts and the trading-period trades, i.e. constant value for each trading period.

Chapter 3

Create FABE

This Chapter presents the creation of the Frequency and Area Balancing Estimator (FABE). FABE is an intra-hour model using available multi-area data. The Chapter is based on [J1], [C1], [C2] and [C3]. Section 3.1 gives a short introduction to the Chapter. Section 3.2 presents the concept available data and how to process low-to-high-resolution data and create an imbalance time-series. Modelling operational dispatch and automatic reserves is presented in algorithms and equations in Section 3.3 and Section 3.4. Finally, Section 3.5 presents frequency and estimated Area Control Error (eACE) calculations.

3.1 Introduction

Different decisions impact on balancing operation can be hard to identify. To identify these decisions impact on SOs goals and missions may be even worse. The purpose of the framework (BEF) is to quantify the impact from many different decisions made at various stages before real-time on selected targets supporting the SOs goals and missions.

The model FABE, illustrated in Figure 3.1, makes it possible to simulate many different decisions. FABE simulates the operation second by second considering the different decisions, the load and production variation, the frequency and the automatic control in the studied system. Also, the structure of FABE makes it possible to test different decisions impact on power system balancing operation using available data.

Available data is multiple bidding zone measurements and schedules from a historical time-period. Depending on the origin of data various data processing methods are applied to transform low-resolution measurements to high-resolution data. This thesis divides the origin of data into fast-regulated production, slow-regulated production, wind power production, consumption, and HVDC-transmission. Gas turbine and reservoir hydro-power production are here referred to as fast-regulated production (FRP) whereas, thermal and run-of-river hydro-power production are

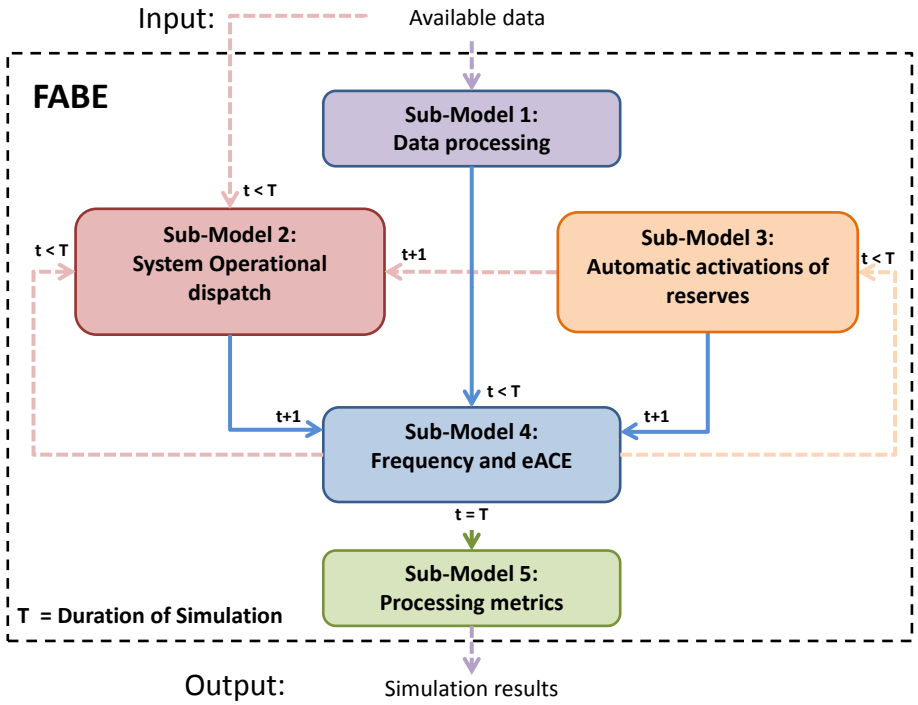

Figure 3.1: Frequency and Area Balancing Estimator (FABE). FABE is divided in five Sub-Models.

referred to as slow-regulated production (SRP). Available frequency response measurements are used to identify system parameters and validate the model.

To capture the normal state frequency and active power dynamics, the model is divided into multiple Sub-Models. Figure 3.1 shows the intra-hour model divided into Sub-Models. First, input data is multi-bidding zone data with several different origins,i.e. FRP, SRP, consumption and HVDC-transmission. Sub-Model 1 processes available data from low-to-high-resolution for a simulation time-period (T). Sub-Model 2 models the system-operational dispatch and uses a five-minute time-scale (k=five min.). Sub-Model 3 activates automatic reserves for the high-resolution time-scale (s=one second). Sub-Model 4 simulates frequency and/or eACE deviations for the high-resolution time-scale (s).

The SOs perspective has been essential building the FABE. Simulation output can either be activated automatic reserves, imbalances, eACE for each area and/or system frequencies. These outputs are refined in Sub-Model 5, described in Chapter 5, to evaluate the balancing performance for different decisions made at various stages before real-time.

This thesis uses 1-second resolution as the needed simulation time-scale (s). The thesis captures the frequency and active power dynamics in the normal state from around one minute. Often one uses 10 times the sample which would imply around 6-10 times higher resolution may be preferable. However, the here used 1-second time-scale will capture frequency deviations accurately enough to measure the power system performance. Nevertheless, the needed simulation time-scale (s) could be changed to 5- or 10-seconds' resolution to lower the number of computations.

3.2 Sub-Model 1: Data processing

Input: data is comparatively low-resolution data, such as hourly measurements (m) for each bidding zone (n) and/or HVDC-transmission line (g); schedules and forecasts of five-minute (k) resolution; and frequency measurements for a specific time-period (T):
$P^{meas.}_{N,M}$, $P^{meas.}_{wN,M}$, $C^{meas.}_{N,M}$, $T^{meas.}_{G,M}$, $P^{plan.}_{N,K}$, $C^{plan.}_{N,K}$, $T^{plan.}_{N,K}$ and $f^{meas.}_{1,S/5}$.

Output: data is high-resolution bidding zone (n) data of needed simulation resolution (s):
$\hat{P}^{base.}_{frn,s}$, $\hat{P}^{meas.}_{srn,s}$, $\hat{P}^{meas.}_{wn,s}$, $\hat{C}^{meas.}_{n,s}$, $\hat{T}^{meas.}_{n,s}$, and $Y_{1,s}$.

Input data is low-resolution trading-period measurements, schedules and forecasts, and frequency measurements.

Trading-period measurements retrieved from [40] had a hourly resolution (m=1h) were active power for all bidding zones (n). Data-measurement origins were production, consumption, wind power production and HVDC-transmissions. Production, consumption and HVDC-transmission schedules and forecasts retrieved from [41] had a five minute resolution (k=5 min.) for all bidding zones. Schedules and forecasts were divided into production, consumption, HVDC-transmission, Re-Scheduled Generation and Tertiary Frequency Control activations. Frequency measurements retrieved from [41] had a five-second resolution ($5s$=5 seconds).

Data of hourly- and five-minute resolution is referred to as low-resolution data, and data of one- and five-second resolution is referred to as high-resolution data (s).

3.2.1 Measurement errors

Measuring and collecting data introduces errors. Chapter 2 defines the imbalance term used in this thesis. However, the measured electrical imbalance is always be zero for a synchronous area. Often, however, measurement errors are resulting in the hourly electrical imbalance (3.1) not being equal to zero.

$$e_{1,m} = \Sigma_1^N (P^{meas.}_{n,m} - C^{meas.}_{n,m} + T^{meas.}_{n,m}) \tag{3.1}$$

The exact cause of these measurement errors is unknown. However, by assuming the hourly measurement errors are mainly caused by inaccurate measured produc-

tion and consumption. By using this assumption, these measurement errors are distributed between production and consumption for each area according to,

$$P_{n,m}^{meas.} - \frac{e_{1,m} P_{n,m}^{meas.}}{\Sigma_1^N (P_{n,m}^{meas.} + C_{n,m}^{meas.})} \rightarrow P_{n,m}^{meas.} \tag{3.2}$$

$$C_{n,m}^{meas.} + \frac{e_{1,m} C_{n,m}^{meas.}}{\Sigma_1^N (P_{n,m}^{meas.} + C_{n,m}^{meas.})} \rightarrow C_{n,m}^{meas.}. \tag{3.3}$$

The new time-series obtained by (3.2) and (3.3) will now satisfy the hourly imbalance (3.1) being equal to zero.

3.2.2 Data-processing methods

Data-processing methods are used to transform available data into high-resolution data. Depending on the origin of data; these methods should re-create the aggregated behaviours in each bidding zone and trading period. To link it to the imbalance definition in Chapter 2; this thesis uses these data-processing methods to re-create the variability within the trading periods. Different data-processing methods are used depending on the origin of data. In this thesis, three different data-processing methods have been developed: K, L and M. Method K transforms fast-regulated production. Method L transforms slow-regulated production, wind power production and consumption. Method M transforms HVDC-transmission. Figure 3.3 illustrate these three different methods.

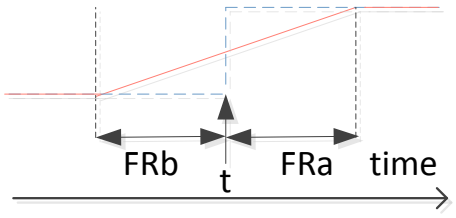

Figure 3.2: Method K. At each step-change at time t, low-to-high-resolution transformations are performed by a ramp starting FRb-minutes before and ending FRa-minutes after a step-change.

Method K (FRP)

Method K is used for fast-regulated production. Fast-regulated production ($P_{frn,m}^{meas.}$) is estimated (3.4) by a system parameter called FR [19]. This is one parameter identified in Section 4.3. Also, often system-operational dispatch, i.e. RSG- and

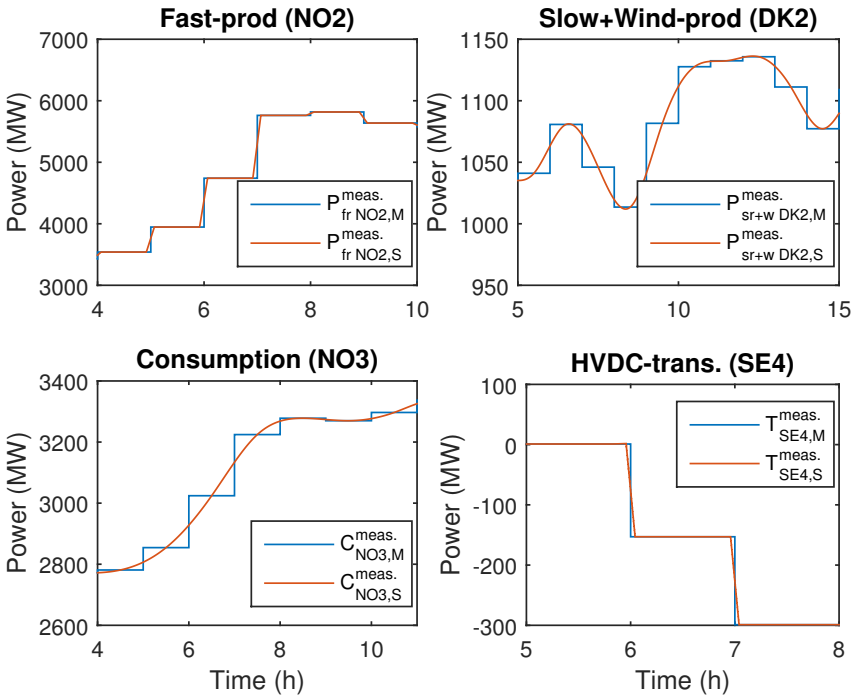

Figure 3.3: Data-processing methods. Upper-left panel shows how Method K transforms fast-regulated production in bidding Zone NO2. Upper-right and lower-left panel shows Method L transforms slow-regulated production, wind power production and consumption in bidding Zone DK2 respective NO3. Lower-right panel shows Method M transforms HVDC-transmission in bidding Zone SE4.

TFC-reserves ($P^{meas.}_{RSGn,k}$, $P^{meas.}_{TFCn,k}$), are fast-regulated production. These decisions are made and planned on five minute resolution (k) and also transformed to high-resolution data by Method K.

$$P^{meas.}_{frN,K} = P^{meas.}_{N,M} * FR \tag{3.4}$$

Method K transforms low-to-high-resolution data into a linear ramp starting FRb-minutes before a step-change and ending FRa-minutes after a step-change. FRa and FRb are set to represent a more realistic step-change of fast-regulated production. Figure 3.2 shows the transformation for one-step change. The method referred to function K(*) in (3.5) transforms data from k-resolution to s-resolution. Figure 3.3 illustrate the transformation for some hours.

$$K(P^{meas.}_{frN,K}) = \hat{P}^{meas.}_{frN,S} \tag{3.5}$$

Method L (SRP, wind production and consumption)

Method L is used for slow-regulated production, wind power production and consumption. Slow-regulated production ($P^{meas.}_{srN,M}$) is estimated (3.6) by a system parameter called FR [19], also used in (3.4). This is a parameter identified in Section 4.3.

$$P^{meas.}_{srN,M} = P^{meas.}_{N,M} * (1 - FR) \tag{3.6}$$

Method L transform low-to-high-resolution data following a cubic spline curve between each step-change. A spline interpolation is preferable to linear interpolation as it gives a smooth and more realistic shape of the fitted curve. It is also preferable to high-order polynomial interpolation as it lowers the oscillations between data points and has a low data-processing error. Spline will minimise the curvature between each data point considering the constraint that the derivate of the first and second order should be equal at each data point for the connecting curves. The cubic spline is the third order spline interpolation. Interpolation methods such as *pchip* [42] was also tested, however, the cubic spline gave the best results.

The low-resolution data values are used in an cubic spline interpolation solution developed by [42]. Low-resolution data is used in-between each step-change, i.e. (m+0.5), as input to the interpolation solution. Method L is referred to as function L(*) in (3.7)-(3.8) transforming data from m-resolution to s-resolution. Figure 3.3 illustrates the transformation for some hours.

$$L(P^{meas.}_{sr/wN,M}) = \hat{P}^{meas.}_{sr/wN,S} \tag{3.7}$$

$$L(C^{meas.}_{N,M}) = \hat{C}^{meas.}_{sr/wN,S} \tag{3.8}$$

Method M (HVDC-transmission)

Method M transforms HVDC-transmission. Different agreements between connected SOs often restricts the ramp rate of HVDC-transmission ($T^{meas.}_{G,M}$). These agreements imply that for each HVDC-transmission line (g) the ramp-rate and the start before and after a step-change can vary. Depending on these agreements the data-processing method can be slightly modified for each line. However, this thesis refers all these transformations as function M(*) in (3.9) transforming data from m-resolution to s-resolution. This method transforms data for each HVDC-transmission line (g) and collects them for each bidding zone (n). Figure 3.3 illustrates the transformation for some hours.

$$M(T^{meas.}_{G,M}) = \hat{T}^{meas.}_{N,S} \tag{3.9}$$

3.2.3 Minimizing the data-processing error

When transforming low-to-high-resolution data using Method K, L and M, an average data-processing error occurs over each trading period (m). The reason for these average data-processing errors is that transformed input data is average measurements. One approach to solve this problem is to develop an optimization method to minimise these data processing errors.

To minimise these errors a practical iterative optimization method has been developed. The objective function to be minimized (3.10) is the error between the average of transformed high-resolution data and low-resolution data,

$$\varepsilon^i = \frac{1}{2}\sum_{n=1}^{N}\sum_{m=1}^{M}(h^i_{n,m})^2, \tag{3.10}$$

where n is the index of bidding zone or line and m is the index of time (m=hourly). $h^i_{n,m}$ is the error in iteration i. $h^i_{n,m}$ can be calculated by equation (3.11) where the index s the interpolated high-resolution index of time (s=1-second). It is the

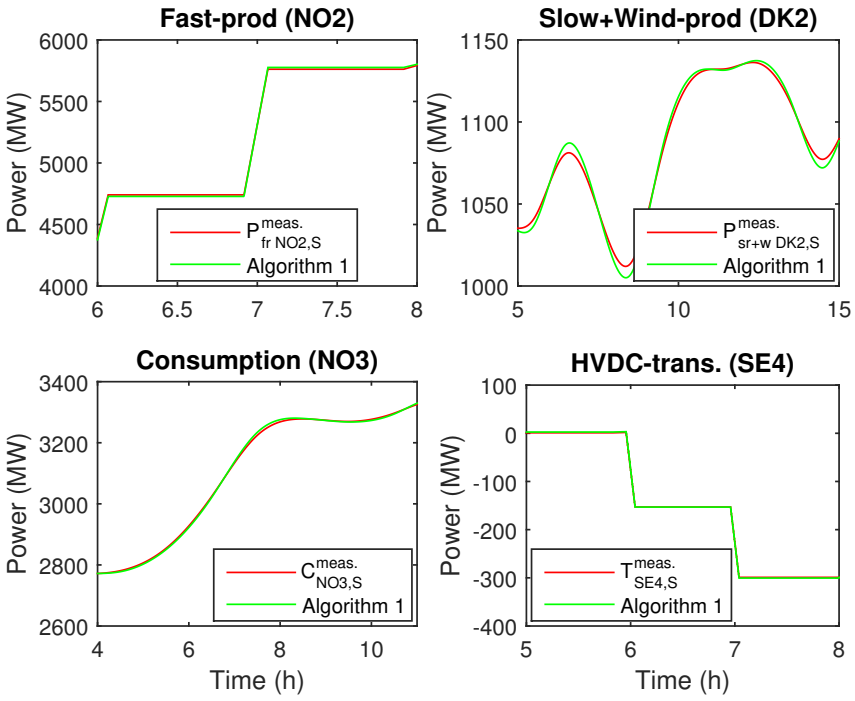

Figure 3.4: Algorithm 1. Minimizing data-processing error and creating new transformed time-series.

trading-period (m) difference between data measurement ($A_{n,m}$) and the transformed high-resolution data ($\hat{A}^i_{n,s}$) for each bidding zone (n) and each iteration (i):

$$h^i_{n,m} = A_{n,m} - \frac{S}{M}\Big(\sum_{s=1+(m-1)\frac{S}{M}}^{m\frac{S}{M}} \hat{A}^i_{n,s}\Big), \tag{3.11}$$

where $S > M$. We use the data-processing Method K, L or M, here referred to as function $f(*)$, to transform low-resolution ($D^i_{n,m}$) to-high resolution data $\hat{A}^i_{n,s}$ in each iteration:

$$\hat{A}^i_{n,s} = f(D^i_{n,m}) \tag{3.12}$$

In the first iteration, the time-series ($D_{n,m}$) is equal to the low-resolution data $A_{n,m}$ according to equation (3.13).

$$D^1_{n,m} = A_{n,m} \tag{3.13}$$

For the next iteration the iteration-variable $D_{n,m}$ will be updated according to the data processing error by equation (3.14).

$$D^{i+1}_{n,m} = D^i_{n,m} + h^i_{n,m} \tag{3.14}$$

The iterative optimization method described in this Subsection is summarized in algorithm 1. The error of high resolution data obtained from algorithm 1 is

Algorithm 1: Method to minimize data-processing errors

Data: Low Resolution data $A_{n,m}$
Result: High Resolution data $\hat{A}^i_{n,s}$
Initialization $D^1_{n,m} = A_{n,m}$
while $\varepsilon^i > \varepsilon_{min}$ *and* $k < k_{max}$ **do**
  Update $D^i_{n,m}, \hat{A}^i_{n,s}, h^i_{n,m}, \varepsilon$:
  $D^{i+1}_{n,m} = D^i_{n,m} + h^i_{n,m}$;
  $\hat{A}^{i+1}_{n,s} = f(D^{i+1}_{n,m})$;
  $h^{i+1}_{n,m} = A_{n,m} - \sum_{1+(m-1)\frac{S}{M}}^{m\frac{S}{M}} \hat{A}^{i+1}_{n,s}$;
  $\varepsilon^{i+1} = \frac{1}{2}\sum_1^N \sum_1^M (h^{i+1}_{n,m})^2$

smaller than using only data-processing methods. Table 3.1 shows how the objective function decreases for some hours and iterations. The results using the method to minimize the data-processing errors indicate that the method is relatively fast. The iterative optimization method to minimize data processing errors was tested on measurements from a historical time-period and results were satisfactory. Figure 3.4 illustrates transformed data using the data processing methods directly and by using the method to minimize the data-processing errors.

Table 3.1: Testing of iterative optimization method

Iteration (IT)	Method K $\frac{1}{2}\sum_1^n\sum_1^m h^2$	Method L $\frac{1}{2}\sum_1^n\sum_1^m h^2$	Method M $\frac{1}{2}\sum_1^n\sum_1^m h^2$
IT1	223	8766	250
IT2	0.5	550	0.01
IT3	-	52	-
IT4	-	5.6	-

3.2.4 Imbalance time-series

To handle imbalances, most power systems have a frequency restoration process [22], [43]. Initially, the inertial response is activated by a difference between mechanical production and electrical consumption. The change in rotating speed and kinetic energy will imply a change in system frequency. First, the frequency change is ceased by activation of Primary Frequency Control (PFC). Secondly, activated PFC is restored by Secondary frequency Control (SFC). Finally, activated PFC and SFC are restored by manual activated Tertiary Frequency Control (TFC) [22, 43]. Also, SOs can act before real-time but after markets gate closure to decrease forecasted imbalances. This is here referred to as the Re-Scheduling of Generation (RSG) process.

Available historical production measurements include measurements of the frequency restoration process and operational dispatches. Following the imbalance definition described in Section 2.5 the frequency restoration process and operational dispatches will handle the variability (V), uncertainty (X) and the difference between forecasts and trades (Z) within each trading period. Following the imbalance definition Section 2.5, the variability is in this thesis defined to be zero over a trading period ($\int_{m-1}^{m} V_m(t)\,\mathrm{d}t = 0$). Thus, the variability is zero over a trading period (m) implying that the average trading-period activations from the frequency restoration process and operational dispatch are equal to the uncertainty and the difference between forecasts and trades ($X_m + Z_m$).

In this thesis, various methods are used to estimate the contribution from the frequency restoration process over each trading period (m). The contribution from TFC and RSG are estimated using schedules from the historical time-period. Contribution from SFC is estimated using measurements from the historical time-period. The contribution from PFC and inertia response is calculated using frequency measurements. Altogether the uncertainty and the difference between forecasts and trades can be calculated (3.15) using these estimated values. It is important to stress; when using historical frequency measurements to calculate the contribution from PFC and inertia response; that it is on low-resolution (m). Otherwise, when using historical frequency measurements to calculate PFC and inertia response the impact on high-resolution results will imply that the high-resolution independence of the two time-series, i.e. simulated frequency and frequency measurements, for model validation and system parameter identification would not be

independent anymore.

$$X_{N,M} + Z_{N,M} = P^{meas}_{_{PFC}N,M} + P^{meas}_{_{SFC}N,M} + P^{meas}_{_{TFC}N,M} + P^{meas}_{_{RSG}N,M} + P^{meas}_{_{iner.}N,M} \tag{3.15}$$

The fast-regulated production time-series subtracted by the contribution of the frequency restoration process are referred to as the base-production ($P^{base}_{frN,M}$). Low-resolution base production time-series (3.16) are calculated for N-areas and for M-trading periods.

$$P^{base}_{frN,M} = P^{meas}_{frN,M} - (X_{N,M} + Z_{N,M}) \tag{3.16}$$

Now; following the imbalance definition described in Section 2.5; the data processing methods described in Section 3.2.2; using the defined fast-regulated base production (3.16); a high-resolution imbalance time-series (3.17) can be calculated. Figure 3.5 shows the high-resolution historical imbalance time-series $Y_{1,S}$ in the lower-panel. Consumption and total production, i.e. base, wind and slow-regulated production, together with HVDC-transmission for a whole synchronous area are shown in the upper panel.

$$Y_{1,S} = \Sigma_1^N(\hat{P}^{base.}_{_{fr}n,S} + \hat{P}^{meas.}_{_{sr}n,S} + \hat{P}^{meas.}_{_{w}n,S} - \hat{C}^{meas.}_{n,S} + \hat{T}^{meas.}_{n,S}) \tag{3.17}$$

The output from Sub-Model 1 is the following high-resolution time-series: Imbalance ($Y_{1,S}$), fast-regulated production ($\hat{P}^{base.}_{_{fr}N,S}$), slow-regulated production ($\hat{P}_{_{sr}N,S}$), wind power production ($\hat{P}_{_{w}N,S}$), consumption ($\hat{C}_{N,S}$), and HVDC-transmission ($\hat{T}_{N,S}$).

3.3 Sub-Model 2: System-operational dispatch

Input: data is scheduled generation, HVDC-transmission between bidding zones; simulated frequency and activated Secondary Frequency Control reserves:
$P^{plan.}_{n,k}$, $C^{plan.}_{n,k}$, $T^{plan.}_{g,k}$, $f^{sim.}(t)$, $eACE^{sim.}(t)$ (see Section 3.5 for details) and $P^{sim.}_{SFC}(t)$.

Output: data is re-scheduled generation one trading period ahead and system-operational-dispatch activations in AT-time from real-time (t):
$P^{sim.}_{RSG}(t+m)$ and $P^{sim.}_{TFC}(t+AT)$.

System-operational-dispatch decisions maintains the normal state operation by restoring, in real-time (t), activated automatic reserves (Sub-Model 3 - Section 3.4) and system variables such as frequency and eACE (Sub-Model 4 - Section 3.5). These decisions are based on information such as forecasts, and real-time (t) simulated frequency, eACE and activated automatic reserves. The modelled processes are not aware of the imbalance time-series (3.17) described in Subsection 3.2.4.

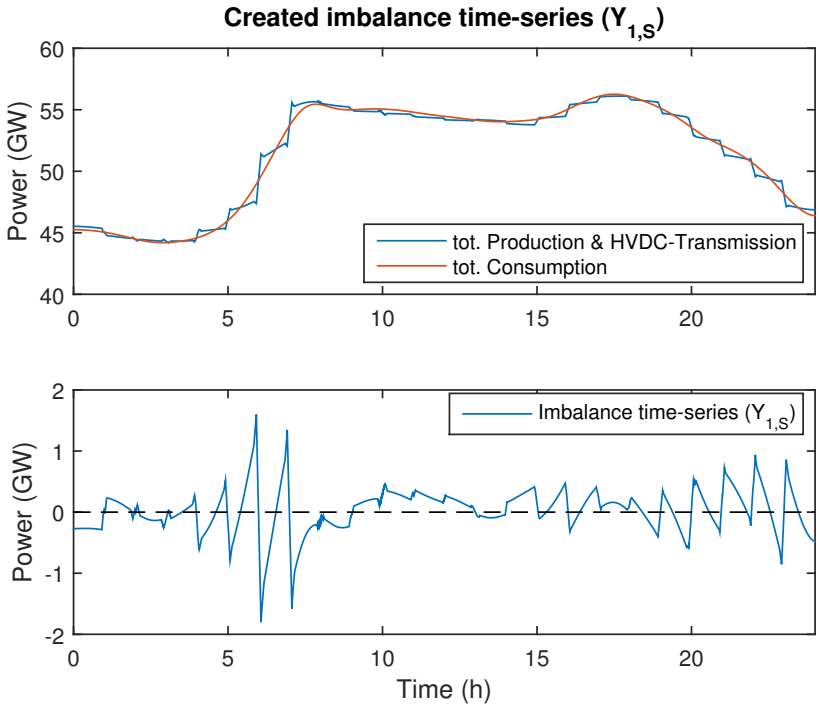

Figure 3.5: A re-created imbalance time-series. Upper-panel shows consumption and the base production together with HVDC-transmission. Lower-panel shows the difference, i.e. the imbalance time-series for the Nordic Synchronous Area during 2016-02-02.

The system-operational dispatch decisions can be seen as one process ending in a decision or various processes ending in many decisions. Figure 3.6 shows how this thesis divides the system-operational dispatch into two decision processes. The first decision process referred to as Re-Scheduling of Generation (RSG) is a decision made once every hour (m-resolution), modelled on time-scale m with decided activations every five minute one hour ahead. The second decision process is the continuously on-going Tertiary Frequency Control (TFC) process modelled on time-scale k. A difference in modelling these two processes is the input data. The RSG-process uses a forecasted imbalances time-series and no measurements whereas the TFC-decisions are based on real-time measurements.

Output data from this Sub-Model are RSG- and TFC-activations transformed from k-resolution to s-resolution using the data processing Method K(*), described in Section 3.2.2.

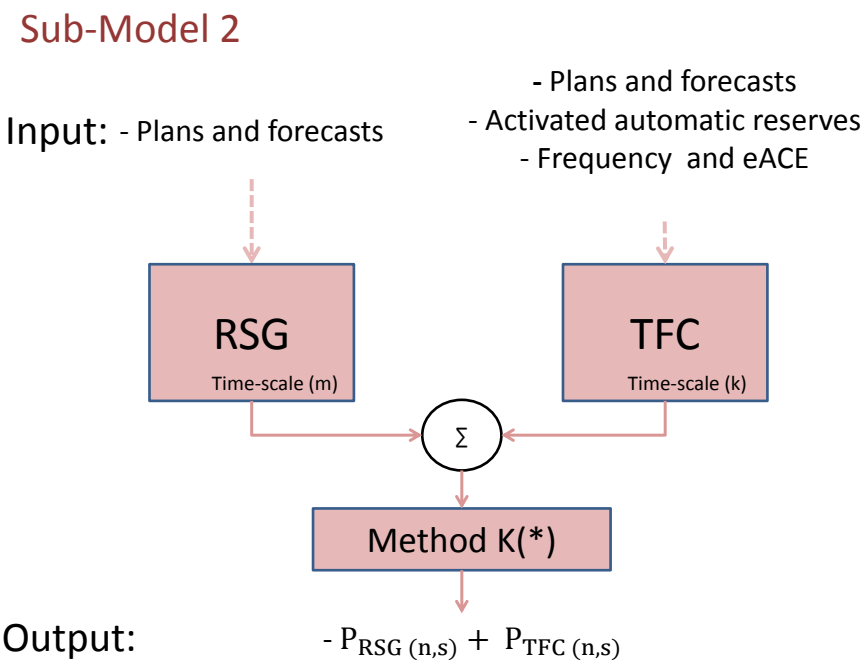

Figure 3.6: Sub-Model 2. Flow-chart of the system-operational-dispatch processes that has been modelled. RSG- and TFC-decisions are transformed from k-resolution to s-resolution by data-processing Method K.

3.3.1 Modelling the RSG-decisions

The RSG-decisions, shown in Figure 3.6, refer here to a re-scheduling of production plans, executed once every hour, 45 minutes before the operating hour starts.

Input data to this process are production plans, planned HVDC-import/export, forecasted consumption and forecasted vRES.

Output data is RSG-scheduled activations of five minute resolution ($P_{RSG_{(K)}}$) for the next trading-period shift.

The goal of this process is to lower frequency deviations around trading-period shifts by distributing production-starts and -stops around each trading-period shift. By combining scheduled production and HVDC-import/export with forecasted consumption and vRES, a forecasted imbalance time-series (3.18) of five-minute resolution are obtained.

The RSG-decisions are modelled by algorithm 2 and can be described as follows. Input data is the RSG confidence factor (K_{RSG}) and the k-resolution forecasted imbalance time-series (3.18), for one hour ahead (m) from the present hour (m+1).

Every hour at $(m + 3k)$; decisions are made of RSG-activations ($P^{sim}_{RSG_{((m+1)\pm 6k)}}$). The decisions are based on the difference between the average forecasted imbalance trading-period-shifts ($\langle Y^{forc}_{(j\pm 6k)} \rangle$) and the forecasted imbalance ($Y^{forc}_{(j\pm 6k)}$), see algorithm 2. The differences are multiplied by a confidence factor ($K_{RSG} \in (0..1)$). Output data is decided RSG-scheduled activations ($P^{sim}_{RSG_{((m+1)\pm 6k)}}$) of k-resolution for the coming hour ($(m + 1) \pm 6k$)).

$$Y^{forc}_{1_{(K)}} = P^{plan}_{(K)} + P^{forc}_{w(K)} - C^{forc}_{(K)} + T^{plan}_{(K)} \tag{3.18}$$

Algorithm 2: Modelled RSG-process once every hour at m+3k

Data: $Y^{forc}_{((m+1)\pm 6k)}$, K_{RSG}

1 $P^{sim}_{RSG_{((m+1)\pm 6k)}} = K_{RSG} * (\langle Y^{forc}_{((m+1)\pm 6k)} \rangle - Y^{forc}_{((m+1)\pm 6k)})$

3.3.2 Modelling the TFC-decisions

The TFC-decisions, shown in Figure 3.6, refer here to a continuously on-going, within operating hours, activation of TFC-reserves.

Input data is a forecasted imbalance time-series, RSG-schedules, and simulated frequency.

Output data is TFC-reserve decisions activated in AT-time.

The TFC-decision process exists in most power systems and restore activated automatic reserves [22]. In many power systems frequency, and/or the Area Control Error (ACE) are the most important control parameters for this process. It is reasonable to use frequency and ACE as they are indicators of activated automatic reserves; and for a synchronous area the system frequency is what ACE is for a balancing area [44]. By using frequency measurements, it is not the frequency's physical value by itself but the implication that frequency deviation is an indicator for activated of PFC-reserves [15, 22]. These manual TFC-reserve activations have an activation time (AT) that is 15 minutes in many power systems [22, 43].

The TFC-decisions are modelled by (3.19) in the time-scale k and can be described as follows. Every five minute (k), a TFC-decision is made. It is activated in 15 minutes ($AT = 3k$) and it is the previous activation ($P_{TFC}(t + (AT - 1k))$) subtracted by the deviation between the control parameter ($f_x(t)$) and the nominal frequency ($f_0 = 50$), times the frequency bias factor (B) and a confidence factor ($K_{TFC} \in (0..1)$).

$$P^{sim}_{TFC}(t + AT) = P_{TFC}(t + (AT - 1k)) + K_{TFC}B(f_x(t) - f_0) \tag{3.19}$$

The control parameter $f_x(t)$ can be changed depending on the TFC dispatch strategy. In this Chapter a control parameter (3.20) calculated by the simulated

frequency ($f^{sim}(t)$) is used. However, in Chapter 5 a new strategy using a more proactive control parameter is modelled.

$$f_x(t) = f^{sim}(t) \tag{3.20}$$

3.4 Sub-Model 3: Activation of automatic reserves

Input: data is simulated frequency and simulated ACE: $f^{sim.}(t)$ and $eACE^{sim.}(t)$.

Output: data is automatic reserve activations: ($P^{sim.}_{PFC}(t)$, $P^{sim.}_{SFC}(t)$).

In all power systems automatic reserves are used. Automatic reserves are important controlling imbalances in synchronous areas and within balancing areas. Usually, these automatic reserves are divided into Primary Frequency Controlled reserves and Secondary Frequency Controlled reserves. Most recently, due to the extensive accommodation of vRES, new types of reserves often called *Ramping Reserves* have been discussed. The purpose of these *Ramping Reserves* is to control highly unpredictable active power ramps causing large imbalances by solar and wind [45]. This new type of reserve is not considered in this thesis.

3.4.1 Primary Frequency Control

Primary Frequency Control (PFC), referred to the normal state Frequency Containment Reserves (FCR-N) used in the Nordic Synchronous Area (NSA). However, PFC reserves exist in all power systems and are a decentralised automatic control that maintains the balance between generation and consumption in a power system using turbine speed governors. This control exists in all power systems. In many power systems, it is fully activated within 30 seconds [22]. In FABE, simulated activations of PFC for all areas (3.21) uses the high-resolution time-scale (s). The PFC activations can be chosen to be a PI controller or being an entire linear based equation. Within this thesis the PFC is modelled according to (3.21). The main reason for this choice is that for the purpose of this framework the equation based model of PFC activations is good enough as their results are very similar in the normal state operation. Figure 3.7 shows simulated results, using FABE, of automatic reserve activations for each area.

$$P^{sim.}_{PFCn}(t) = (f^{sim.}_n(t) - f_0) * PFC_n \tag{3.21}$$

3.4.2 Secondary Frequency Control

Secondary Frequency Control (SFC), referred to the aFRR reserve in the NSA, is a centralised automatic control that brings frequency back to its target value. The control exists in all large interconnected systems where TFC does not remove overloads on tie-lines quickly enough. In many synchronous areas it is fully activated

within 10-15 minutes [22]. SFC is usually used to bring ACE back to zero. Nevertheless, the exact design of SFC varies between areas [22]. The principle of the Network Characteristic Method (3.22) is to minimize the real-time Area Control Error (ACE) [43]. The tuning of these parameters has not been performed here. However, the proportional parameter (p_n) should not be excessively large [43] and the integrating parameter (T_n) should be limited in case of persisting positive or negative ACE values [43]. However, SFC is not always in use in NSA, and Figure 3.7 shows simulation results using FABE for a specific day when SFC was not activated.

$$P^{sim.}_{SFCn}(t) = -p_n * eACE^{sim.}_n(t) - \frac{1}{T_n}\int eACE^{sim.}_n(t) * dt \tag{3.22}$$

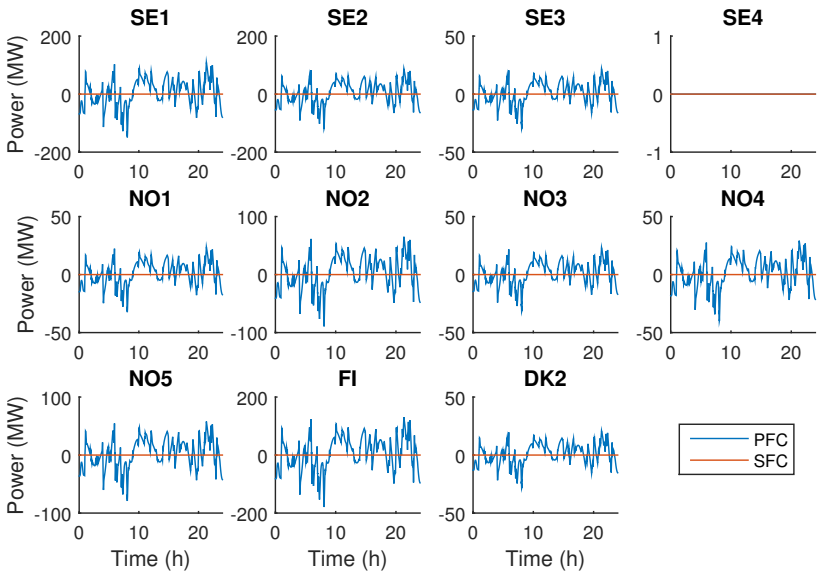

Figure 3.7: Simulated results of activations of automatic reserves for all bidding zones using FABE for the Nordic Synchronous Area during 2016-02-02.

3.5 Sub-Model 4: Frequency and eACE

Input: data for each bidding zone (n) is: $\hat{P}^{base.}_{frn}(t)$, $\hat{P}^{meas.}_{srn}(t)$, $\hat{P}^{meas.}_{wn}(t)$, $P^{sim.}_{SFCn}(t)$, $\hat{P}^{sim.}_{TFCn}(t)$, $\hat{P}^{sim.}_{RSGn}(t)$, $P^{plan}_{frn}(t)$, $P^{plan}_{srn}(t)$, $P^{plan}_{wn}(t)$, $P^{plan}_{TFCn}(t)$, $P^{plan}_{RSGn}(t)$, $\hat{C}^{meas.}_n(t)$, $C^{plan}_n(t)$, $\hat{T}^{meas.}_n(t)$, $T^{plan}_n(t)$, $P^{sim.}_{PFCn}(t)$, $P^{sim.}_{SFCn}(t)$, $\hat{P}^{sim.}_{TFCn}(t)$, $\hat{P}^{sim.}_{RSGn}(t)$, and $Y(t)$.

Output: data is: $f^{sim.}(t)$ and $eACE^{sim.}(t)$.

System frequency is simulated by (3.23) and (3.25) in the high-resolution time-scale (s). First, inertial response ($P^{sim.}_{iner.n,s}$) is calculated by,

$$P^{sim.}_{iner.}(t) = Y(t) + \Sigma_1^N (P^{sim.}_{PFCn}(t) + P^{sim.}_{SFCn}(t) + \hat{P}^{sim.}_{TFCn}(t) + \hat{P}^{sim.}_{RSGn}(t)). \quad (3.23)$$

Frequency deviations can, for a system with highly meshed grid, be modelled by a linearized aggregated swing equation (3.24) [46]. Here the assumption of a constant value of the kinetic energy ($H_{sys.}S_{sys.}$) is used.

$$\frac{df}{dt}^{sim.} = -\frac{f_0 - f^{sim.}(t)}{2H_{sys.}S_{sys.}D_{load}} f_0 + \frac{P^{sim.}_{iner.}(t)}{2H_{sys.}S_{sys.}} f_0 \quad (3.24)$$

this thesis investigate comparatively small and slow frequency deviations during the normal state operation. Considering this, the first term on the right hand side in (3.24) can be neglected. This assumption may not be used if we examined frequency stability during contingencies. Frequency deviation is then here represented by,

$$\frac{df}{dt}^{sim.} = \frac{P^{sim.}_{iner.}(t)}{2H_{sys.}S_{sys.}} f_0. \quad (3.25)$$

ACE is defined as the difference between an area's planned and measured flow between the actual bidding zone and its adjacent bidding zones ($\Delta L_{n,s}$) subtracted by each bidding zone's activated PFC (3.26) [47]. FABE define positive flow towards its neighbours as:

$$ACE_n(t) = \Delta L_n(t) - P^{sim.}_{PFCn}(t). \quad (3.26)$$

This thesis does not calculate power-flows over AC tie-lines: each area's total flow over AC tie-lines is estimated by each area's difference between measured and planned generation, consumption, and HVDC-transmission together with the areas activated automatic reserves,

$$\begin{aligned}\Delta L_n(t) =& ((\hat{P}^{base.}_{frn}(t) + \hat{P}^{meas.}_{srn}(t) + \hat{P}^{meas.}_{wn}(t) + P^{sim.}_{SFCn}(t) + \hat{P}^{sim.}_{TFCn}(t) + \hat{P}^{sim.}_{RSGn}(t)) \\ & - (P^{plan}_{frn}(t) + P^{plan}_{srn}(t) + P^{plan}_{wn}(t) + P^{plan}_{TFCn}(t) + P^{plan}_{RSGn}(t))) \\ & - (\hat{C}^{meas.}_n(t) - C^{plan}_n(t)) + (\hat{T}^{meas.}_n(t) - T^{plan}_n(t)) + P^{sim.}_{PFCn}(t).\end{aligned} \quad (3.27)$$

In this thesis, modelled TFC- and RSG-decisions in FABE aims to balance the power system. TFC- and RSG-decisions made for balancing the system should not affect the particular bidding zone ACE and are included in (3.27). TFC-decisions made for balancing a specific bidding zone and/or congestions between bidding zones these schedules should not be included in (3.27). In the NSA, TFC-decisions for balancing a specific bidding zone are referred to as *special* TFC-decisions whereas the decisions included in this thesis are referred to as *balancing* TFC-decisions [29].

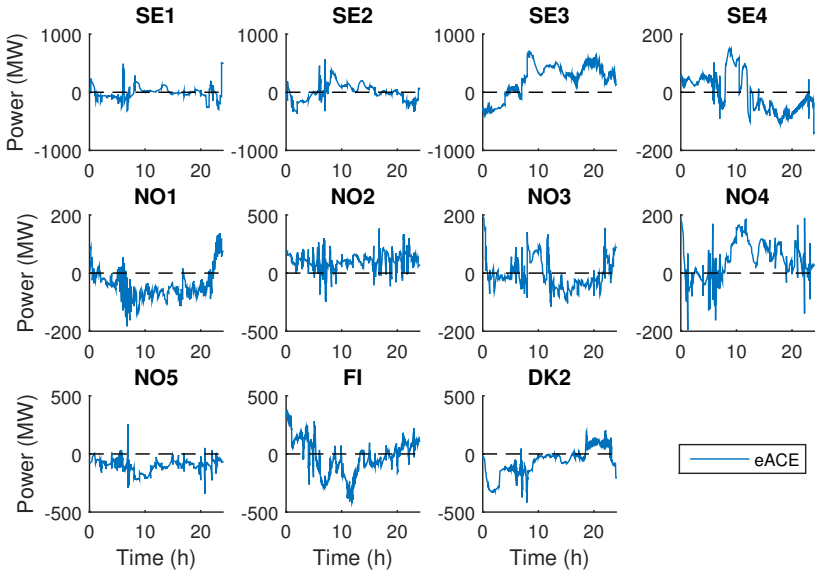

Figure 3.8: Simulated results of estimated Area Control Error (eACE) for all bidding zones using FABE for the Nordic Synchronous Area during 2016-02-02.

By combining (3.26) and (3.27) ACE can be estimated (eACE), shown in Figure 3.8 by,

$$\begin{aligned} eACE_n^{sim.}(t) \\ =&((\hat{P}_{fr\,n}^{base.}(t) + \hat{P}_{sr\,n}^{meas.}(t) + \hat{P}_{w\,n}^{meas.}(t) + P_{SFC\,n}^{sim.}(t) + \hat{P}_{TFC\,n}^{sim.}(t) + \hat{P}_{RSG\,n}^{sim.}(t)) \\ &- (P_{fr\,n}^{plan}(t) + P_{sr\,n}^{plan}(t) + P_{w\,n}^{plan}(t) + P_{TFC\,n}^{plan}(t) + P_{RSG\,n}^{plan}(t))) \\ &- (\hat{C}_n^{meas.}(t) - C_n^{plan}(t)) + (\hat{T}_n^{meas.}(t) - T_n^{plan}(t)). \end{aligned} \tag{3.28}$$

Chapter 4

FABE validation and system parameter identification

This chapter presents intra-hour model validation and system parameter identifications. This chapter is based on [J1], [C1] and [C3]. Section 4.1 gives a short introduction to the Chapter. Section 4.2 identifies system parameters, such as primary frequency control reserve capacities (PFC^{cap}) and parameters used in data-processing methods, previously described in Section 3.2. Section 4.3 validates the model using various validation methods based on normal state measurements. Section 4.4 presents the reference scenario called Base Case (BC).

4.1 Introduction

Chapter 3 presented a work-flow methodology to build and create an intra-hour model here referred to as FABE. In this thesis FABE uses available data from a historical time-period. An advantage using historical data is that system parameters can be identified and that the model can be validated using independent measurements.

In most power systems, active power in trading-period resolution and frequency in high-resolution are measured. An important reason when developing the idea of the work leading to this thesis is that these data time-series are independently measured and often publicly available. These independent measurements can be used to identify system parameters and validate FABE. Available data used in this thesis is; average hourly measurements of production, consumption and HVDC-transmission from a historical time-period retrieved from [40], and schedules, forecasts and frequency measurements retrieved from [41].

A training set and a validation set are created separating available data into two sets of time-series. Separated data sets are essential to overcome over-fitting issues. This thesis proposes to use 50 percent of the data for the training set and 50 percent of the remaining data for the validation set. An indication of model

over-fitting is inconsistencies between RMSE results between measurements and simulated frequencies obtained using the different data sets [48]. Figure 4.1 shows how the two data sets are separated to identify system parameters and validate the model set-up.

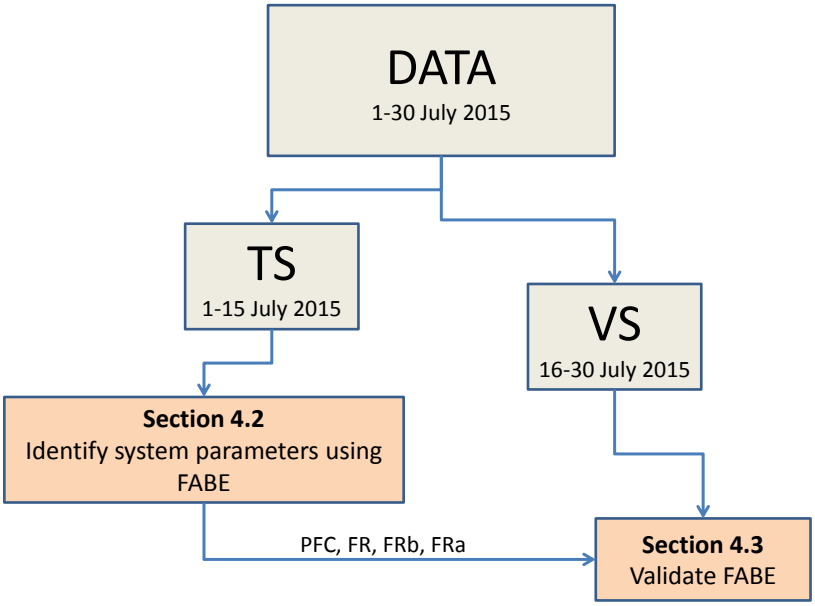

Figure 4.1: Data from a historical time-period is divided into two data-sets to identify system parameters and validate the model set-up.

Various methods are used for system parameter identification and model validation in Section 4.2 and Section 4.3. In the next Chapter, the validated model and identified system parameters are referred to as Base Case (BC). Base Case is used as a reference scenario when investigating and analysing new decisions in Chapter 5.

4.2 Identify system parameters with FABE

The purpose of the system parameter identification is to verify known and/or to identify unknown parameters in the normal state operation. To identify system parameters one can use different approaches. One approach is to identify system parameters, such as the primary frequency control capacity, is to use high-resolution

measurements and simulated frequencies during a contingency [31, 32]. This approach may be accurate enough for models used for contingency analyses. However, for models used to mimic the normal state operation several non-linearities such as generation and HVDC disturbed mode activations, generation units reaching their maximum output limitations, and load voltage- and frequency-dependencies, all have an unwanted impact on these identified system parameters.

The approach developed in this thesis is to identify normal state system parameters based on high-resolution simulated and frequency measurements during normal state operation. By analysing these time-series using different statistical tools, we can identify system parameters and validate the model for the normal state operation.

4.2.1 Identifying primary frequency control capacities

The Primary Frequency Control capacities (PFC^{cap}) are not always known. A reason for this is that the PFC reserves, described in Section 3.4.1, is a decentralised automatic reserve and the system operators may not have the information from all power plants if it is provided or not.

To estimate PFC^{cap} one can use different approaches [45, 49, 50]. Two separate methods have been developed and used in this thesis.

Method A, estimates PFC^{cap} for the synchronous area including the load frequency-dependency based on simulated frequencies and frequency measurements. The simulated high-resolution frequencies are obtained using FABE.

Method B estimates PFC_n^{cap} for each bidding zone not including the load frequency-dependency based on the difference, in trading-period resolution (m), between frequency deviation and the difference between measured and scheduled production.

Method A: Estimating the primary frequency control capacity based on frequency measurements and simulated frequencies

One approach to estimate PFC^{cap}, developed in this thesis, is based on frequency measurements and simulated frequency response using FABE for a certain time-period (T). The problem formulation (4.1) to estimate the primary frequency control capacity based on frequency measurements and simulated frequency response. The method estimates the scalar PFC^{cap} by minimizing the objective function changing the variable PFC^{cap} used in fabe(*).

$$\begin{aligned} \underset{PFC}{\text{minimize}} \quad & \frac{1}{2}\Sigma_{t=1}^{T}((\sigma(f_t^{sim.}) - \sigma(f_t^{meas.}))^2 \\ \text{subject to} \quad & f_T^{sim.} = fabe(PFC^{cap}) \end{aligned} \tag{4.1}$$

Method A (4.1) can also be described as follows.

· The objective function to be minimised is the difference between the standard deviation of simulated frequency ($\sigma(f^{sim.})$), obtained using FABE, and frequencies measurements ($\sigma(f^{meas.})$), retrieved from [41]. The time-period can be changed; however, this thesis has tested the method using a time-period (T) of 15 days.

$$\frac{1}{2}(\sigma(f_T^{sim.}) - \sigma(f_T^{meas.}))^2 \tag{4.2}$$

· It is subjected to one constraint.

a) The simulated frequency response should be obtained using FABE, referred here to the function $fabe(*)$. The variable used in FABE is the primary frequency response capacity (PFC^{cap}).

$$f_T^{sim.} = fabe(PFC_T^{cap}) \tag{4.3}$$

To solve the problem (4.1) a practical optimization approach has been developed. The objective function to be minimized (4.4) is the squared difference between the standard deviation of the simulated and measured frequencies for a time-period (T),

$$J^A = \frac{1}{2}(\sigma(f_T^{sim.}) - \sigma(f_T^{meas.}))^2. \tag{4.4}$$

The simulated frequency ($f_T^{sim.}$) is obtained using FABE. Input data to FABE is low-resolution measurements from that time-period. These data time-series is constant for all iterations, and the input variable to FABE here, is the PFC reserve capacity (PFC^{cap}).

In the first iteration (4.5), the PFC reserve capacity is equal to 6000 $\frac{MW}{Hz}$, which is the NSA's grid code requirement [51].

$$PFC^{cap,1} = 6000 \tag{4.5}$$

For the next iteration the simulated frequency response ($f_T^{sim.,(i+1)}$) will be updated using FABE, and the direction for the next iteration (d^i) will be updated according to,

$$d^i = \sigma(f_T^{sim.,(i)}) - \sigma(f_T^{meas.,(i)}). \tag{4.6}$$

The next iteration variable ($PFC^{cap,(i+1)}$) will be updated according to equation (4.7) using the step length ($\gamma \in Z^+$). The step length can be chosen empirical or using the objective functions. The later can speed up the iteration time; however within this thesis it has not been necessary.

$$PFC^{cap,(i+1)} = PFC^{cap,i} - \gamma d^i, \tag{4.7}$$

Algorithm 3 illustrates the practical optimization method to estimate the primary frequency control capacity based on simulated frequency and frequency measurements.

Algorithm 3: Method A

Data: $f_T^{meas.}, \gamma$
Result: PFC reserve capacity PFC^{cap}
Initialization PFC=6000 $\frac{MW}{Hz}$
while $J^{A,i} > J^A_{min}$ *and* $i < i_{max}$ **do**
  Update $PFC^{cap,i}, f_T^{sim.,i}, J^{A,i}$:
  $d^i = \sigma(f_T^{sim.,(i)}) - \sigma(f_T^{meas.,(i)})$;
  $PFC^{cap,(i+1)} = PFC^{cap,i} - \gamma d^i$;
  $f_T^{sim.,(i+1)} = fabe(PFC^{cap,(i+1)})$;
  $J^{A,(i+1)} = \frac{1}{2}(\sigma(f_T^{sim.,(i+1)}) - \sigma(f_T^{meas.,(i+1)}))^2$

Method B: Estimating PFC_n^{cap} based on scheduled & measured production and frequency measurements

In order to identify PFC_n^{cap} for each bidding zone (n), one can analyse frequency deviation and the difference between scheduled production and production measurements over several trading periods. The scheduled production data, retrieved from [41], were the SOs latest schedules from that time-period and the production measurements were retrieved from [40]. In contrast to Method A; Method B does not consider the frequency dependence of load; implying, results from Method B should be lower than results obtained with Method A. However, in contrast to Method A; Method B can be used to estimate PFC^{cap} for each bidding zone. The Method B problem formulation (4.8) have been developed to estimate the primary frequency controlled capacities for each bidding zone (n).

$$\begin{aligned} \underset{a,b}{\text{minimize}} \quad & \Sigma_{m=1}^{M} \frac{1}{2}(y_{n,m} - a_n - b_n x_{n,m})^2 \\ \text{subject to} \quad & x_{n,m} = f_m^{meas.} - f_0 \ \forall m \\ & y_{n,m} = P_{n,m}^{plan} - P_{n,m}^{meas.} \ \forall m \end{aligned} \tag{4.8}$$

The problem (4.8) can be described as follows.

· The objective function to be minimized is a linear regression set-up using variable a and b. Variable a is the linear regression offset parameter and b is the slope parameter indicating each bidding zone's (n) PFC-capacity.

$$\frac{1}{2}(y_{n,m} - a_n - b_n x_{n,m})^2 \tag{4.9}$$

· It is subjected to two constraints.

a) X-coordinate should be equal to frequency measurements on hourly resolution m ($f_m^{meas.}$), subtracted by the nominal frequency (f_0) for all

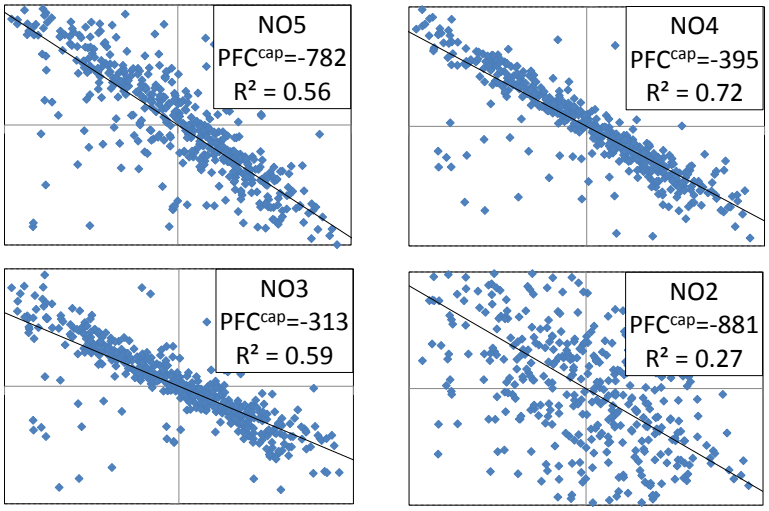

Figure 4.2: Method B: Estimating primary frequency controlled capacities based on scheduled and measured production during 1-15 of July 2015. X-axes shows frequency deviation (Hz) and y-axes shows active power (MW).

hourly samples (m).

$$x_{n,m} = f_m^{meas.} - f_0 \tag{4.10}$$

b) Y-coordinate should be equal to the difference between scheduled and production measurements for each bidding zone (n) and for all hourly samples (m).

$$y_{n,m} = P_{n,m}^{plan} - P_{n,m}^{meas.} \tag{4.11}$$

The problem (4.8) has been solved using FABE and linear regression. Figure 4.2 and 4.3 show results using Method B. Method B can estimate PFC_n^{cap} with high confidence for many bidding zones. Results from testing the method on the data for the Nordic Synchronous Area from 1-15 of July 2015 were satisfactory for NO1, NO3, NO4 and NO5. However, for NO2 it was not as good, and for all other bidding zones, the results were not useful.

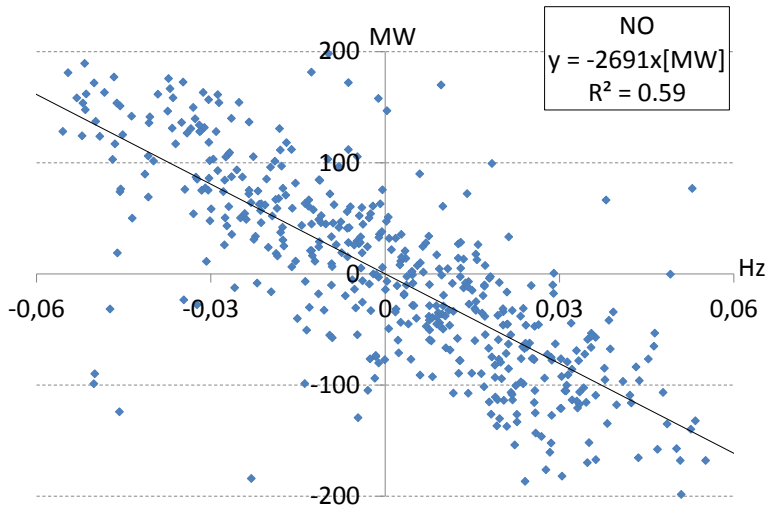

Figure 4.3: Estimating primary frequency controlled capacities based on scheduled and measured production during 1-15 of July 2015 for Norway using Method B (4.8).

4.2.2 Identifying data-processing-methods parameters

This thesis uses data-processing methods to transform low-to-high-resolution data. These methods use various parameters, and some are unknown. In order to identify these parameters two independent time-series of frequency response are used. The first time-series is measured high-resolution frequency response and the second time-series is simulated frequency response using FABE. Input data to FABE are low-resolution measurements for each bidding zone described in Chapter 3.

In order to identify the data-processing-methods parameters this thesis uses the Pearson's correlation coefficient between simulated and frequency measurements for a historical time-period (T). Pearson's correlation coefficient is the covariance of the two time series divided by the product of their standard deviations.

A correlation problem formulation (4.12) to identify parameters used in the data-processing-methods have been developed.

$$\begin{aligned} \underset{FR,FRa,FRb}{\text{maximize}} \quad & r(f_T^{meas.}, f_T^{sim.}) \\ \text{subject to} \quad & f_T^{sim.} = fabe(FR, FRa, FRb) \end{aligned} \tag{4.12}$$

The problem formulation (4.12) can also be described in the following way.

- The objective function to be maximised is the Pearson's correlation coefficient (r) between high-resolution measurements and simulated frequencies over a simulation time-period (T).

$$r(f_T^{meas.}, f_T^{sim.}) \tag{4.13}$$

- It is subjected to one constraint.

  a) Simulated frequency response should be obtained using FABE, here referred to as function $fabe(*)$. Input variables are FR, FRa, and FRb.

$$f_T^{sim.} = fabe(FR, FRa, FRb) \tag{4.14}$$

A practical optimization approach have been developed to solve the correlation problem (4.12). The objective function to be maximised (4.15) is the Pearson's correlation coefficient between simulated and frequency measurements for a historical time-period (T),

$$J^P = r(f_T^{meas.}, f_T^{sim.}). \tag{4.15}$$

The simulated frequency ($f_T^{sim.}$) of resolution (5s) is obtained using FABE. The reason for the five seconds resolution is that the sampled frequency measurements, retrieved from [41], are of five-second resolution. Input data to FABE is low-resolution (m) measurements for each bidding zone from that time-period. These data time-series are constant through all iterations; however, unknown variables are some parameters in the data-processing methods. The parameters to identify are FR, FRa and FRb, described in Chapter 3.

In the first iteration, FR, FRa and FRb are reasonable best guess values. Reasonable best guess values can differ between power systems and areas. However, for the NSA, the best guess has been found impractically, and FR, FRa and FRb was set to 80, 5 and 5 respectively, according to (4.16).

$$\begin{bmatrix} FR^1 & FRb^1 & FRa^1 \end{bmatrix} = \begin{bmatrix} 80 & 5 & 5 \end{bmatrix} \tag{4.16}$$

For the next iteration the simulated frequency response ($f_T^{sim.,(i+1)}$) will be updated using FABE, and the direction for the next iteration (d^i) will be updated according to,

$$d^i = \begin{bmatrix} \frac{\partial J^P}{\partial FR^i} & \frac{\partial J^P}{\partial FRb^i} & \frac{\partial J^P}{\partial FRa^i} \end{bmatrix}. \tag{4.17}$$

Algorithm 4: Identifying parameters used in data processing methods

Data: $f_T^{meas.}, \gamma$

Result: Identified parameters: FR, FRb, FRa

Initialization $\begin{bmatrix} FR^1 & FRb^1 & FRa^1 \end{bmatrix} = \begin{bmatrix} 80 & 5 & 5 \end{bmatrix}$

while $J^{P,i} > J^P_{min}$ *and* $i < i_{max}$ **do**

  Update $\begin{bmatrix} FR^i & FRb^i & FRa^i \end{bmatrix}, f_T^{sim.,i}, J^{P,i}$:

  $d^i = \begin{bmatrix} \frac{\partial J^P}{\partial FR^i} & \frac{\partial J^P}{\partial FRb^i} & \frac{\partial J^P}{\partial FRa^i} \end{bmatrix}$;

  $\begin{bmatrix} FR^{(i+1)} & FRb^{(i+1)} & FRa^{(i+1)} \end{bmatrix} = \begin{bmatrix} FR^i & FRb^i & FRa^i \end{bmatrix} + \gamma d^i$;

  $f_T^{sim.,(i+1)} = fabe(FR^{(i+1)}, FRb^{(i+1)}, FRa^{(i+1)})$;

  $J^P = r(f_T^{meas.}, f_T^{sim.,(i+1)})$

The gradients (∇J^P) for each iteration (i) are found numerically using FABE together with each variable one by one, changed by adding and subtracting a small value ($\pm\epsilon$) according to,

$$\frac{\partial J^P}{\partial FR^i} = \left[\frac{J^P(FR^i+\epsilon) - J^P(FR^i-\epsilon)}{2\epsilon} \right], \tag{4.18}$$

$$\frac{\partial J^P}{\partial FRb^i} = \left[\frac{J^P(FRb^i+\epsilon) - J^P(FRb^i-\epsilon)}{2\epsilon} \right], \tag{4.19}$$

$$\frac{\partial J^P}{\partial FRa^i} = \left[\frac{J^P(FRa^i+\epsilon) - J^P(FRa^i-\epsilon)}{2\epsilon} \right]. \tag{4.20}$$

For the next iteration the variables ($FR^{(i+1)}, FRb^{(i+1)}, FRa^{(i+1)}$) will be updated according to equation (4.21) using the step length ($\gamma \in Z^+$). The step length can be chosen empirical or using the objective function. The later can speed up the iteration time; however within this thesis it has not been necessary.

$$\begin{bmatrix} FR^{(i+1)} & FRb^{(i+1)} & FRa^{(i+1)} \end{bmatrix} = \begin{bmatrix} FR^i & FRb^i & FRa^i \end{bmatrix} + \gamma d^i \tag{4.21}$$

Algorithm 4 illustrates the practical optimization method to identify data-processing-methods parameters.

4.2.3 Results

In order to identify the normal state power system parameters; data from the Nordic Synchronous Area for 1-15 January and 1-15 July have been used. Results are compiled in Table 4.1. For the model validation, these identified system parameters together with data from the next 15 days in July and January have been used in Section 4.3.

Table 4.1 shows identified system parameters for the Nordic Synchronous Area for the first 15 days of January and July 2015. Results indicate that the identified system parameters are quite similar for the tested time-periods except for

the primary frequency control capacity (PFC^{cap}). The primary frequency control capacity is interestingly increased in January compared to July. These results are in line with the general belief that increased hydro-power production increases the amount of PFC reserve capacities; although the grid code requirement is 6000 (MW/Hz).

Table 4.2 summarises the results using (4.8). The results were satisfactory with very good R2 values for NO1, NO3, NO4 and NO5 and quit good for NO2 however, for the other bidding zones results were not good at all.

These identified system parameters are from here on used for model validation and the reference scenario BC.

Table 4.1: Identified normal state power system parameters using (4.1) and (4.12) during 1-15 of July respective 1-15 of January, 2015.

Time-period	Method A	Data processing methods parameters		
15 days	PFC^{cap} (MW/Hz)	FRa (min.)	FRb (min.)	FR (%)
January 2015	-7200	4.3	4.8	74
July 2015	-6200	4.2	5.1	78

Table 4.2: Identified primary frequency controlled capacities using (4.8) during 1-15 of July, 2015.

	Method B	
Bidding zone	PFC_n^{cap} (MW/Hz)	R2
NO1	-320	0.73
NO2	-882	0.27
NO3	-313	0.59
NO4	-395	0.72
NO5	-782	0.56
Total NO:	-2691	0.59
SE1, SE2, SE3, SE4, DK2, FI	-	0

4.3 Validate FABE

Validation is a task demonstrating a model's reasonable representation of the actual system, i.e. the model should be able to reproduce system behaviours with enough fidelity to satisfy analysis objectives [52].

It is performed to understand the underlying power system phenomena so they can be appropriately represented. Model validation often requires "engineering judgment" rather than being based on a simple pass or fail criteria [53]. A method to validate models is to analyse frequency responses during contingencies [31, 32].

However, this model has been developed to analyse the normal state active power and frequency dynamics. Therefore, the model fidelity should be evaluated on how well it can reproduce system frequency behaviours in the normal state operations. Also, when validating the model, awareness of the assumptions creating the model is essential.

Assumptions creating the model are the following. The primary assumption is that available low-resolution data can be transformed into high-resolution data to represent true system behaviours. It includes reducing measurements errors, different data-processing methods depending on the origin of data, and re-creating a historical imbalance time-series using scheduled and calculated RSG, TFC and automatic reserve activations, described in Section 3.2.

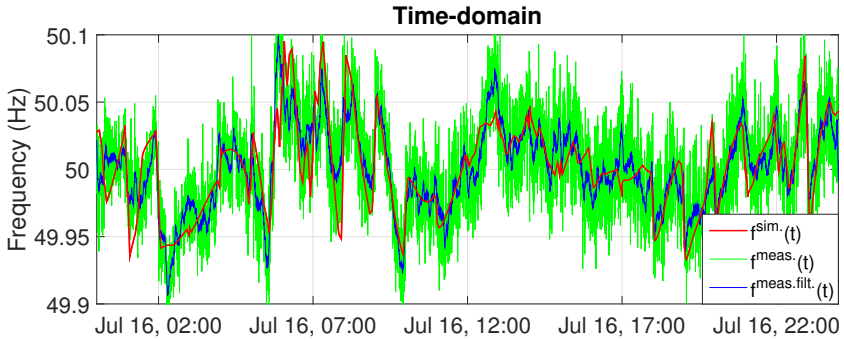

Figure 4.4: Frequency responses. Simulated frequency ($f^{sim.}(t)$) and frequency measurements ($f^{meas.}(t)$). A first-order low-pass filter creates the filtered frequency measurement ($f^{meas.filt.}(t)$) using a time constant of 60 seconds.

Table 4.3: **Validation 1**. R2 and RMSE using data from 16-30 of July 2015.

Average values of resolution (t)	R2($f_t^{meas.}$,$f_t^{sim.}$)	RMSE($f_t^{meas.}$,$f_t^{sim.}$)
1 sec.	0.72	0.019

To validate a model the best method is to use real-time measurements [52]. An important reason when starting developing this model was that often high-resolution frequency measurements are available making it possible to validate appropriate real power systems normal state behaviours. Therefore model validation is performed comparing simulated high-resolution frequency model output and the independent high-resolution frequency measurements from the same time-period. Figure 4.4 illustrates simulated frequency and frequency measurements for a particular day.

Rather than merely pass or fail this thesis compares the two time-series with different approaches visualising different aspects of system behaviours. Four different validation methods have been used.

Validation 1: Two statistical tools have been used.

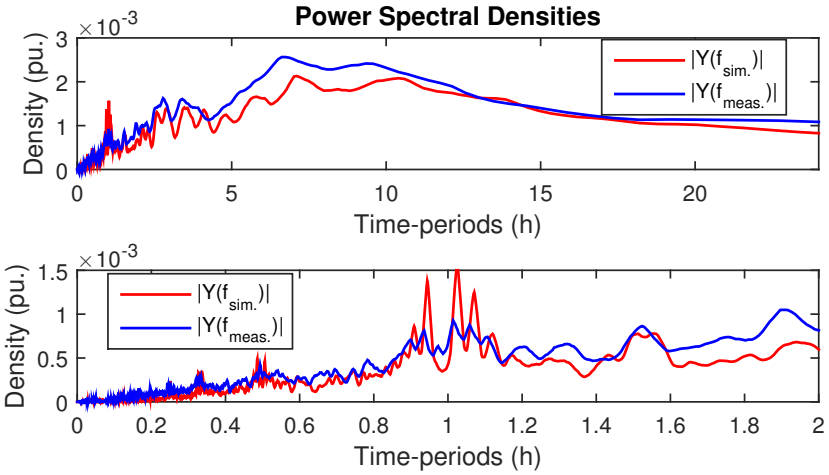

Figure 4.5: **Validation 2**. Power spectral densities for simulated frequency and frequency measurements using data from 16-30 of July 2015. Fast-Fourier Transformation (FFT) transforms frequency time-series to frequency domain [1]. The upper-panel shows power spectral densities from 0 to 24 hours. The lower-panel shows power spectral densities from 0 to 2 hours.

The first tool is the RMSE value,

$$RMSE = \sqrt{\frac{\Sigma_{t=1}^{T}(f_t^{meas.} - f_t^{sim.})^2}{T}}. \tag{4.22}$$

The RMSE value is useful indicating the standard deviation of the difference between the model's simulated frequency output and the independent frequency measurements.

The second tool is the coefficient of determination (R^2),

$$R^2 = 1 - \frac{\Sigma_{t=1}^{T}(f_t^{meas.} - f_t^{sim.})^2}{\Sigma_{t=1}^{T}(f_t^{meas.} - 50)^2}. \tag{4.23}$$

The R^2 value indicates how well the model's simulated frequency output predicts the variance of the independent frequency measurements. Table 4.3 compiles the results for 16-30 July 2015, using identified system parameters from 1-15 of July.

Validation 2: This thesis evaluates the power spectral densities of simulated and frequency measurements. The power spectral densities have been created using

simulated frequency and frequency measurements. The power spectral densities describe the distribution of power into frequency components composing those signals [54]. Figure 4.5 shows the resulted power spectral densities for 16-30 July 2015, using identified system parameters from 1-15 of July. The upper panel shows power spectral densities from 0 to 24 hours and the lower-panel shows power spectral densities from 0 to 2 hours.

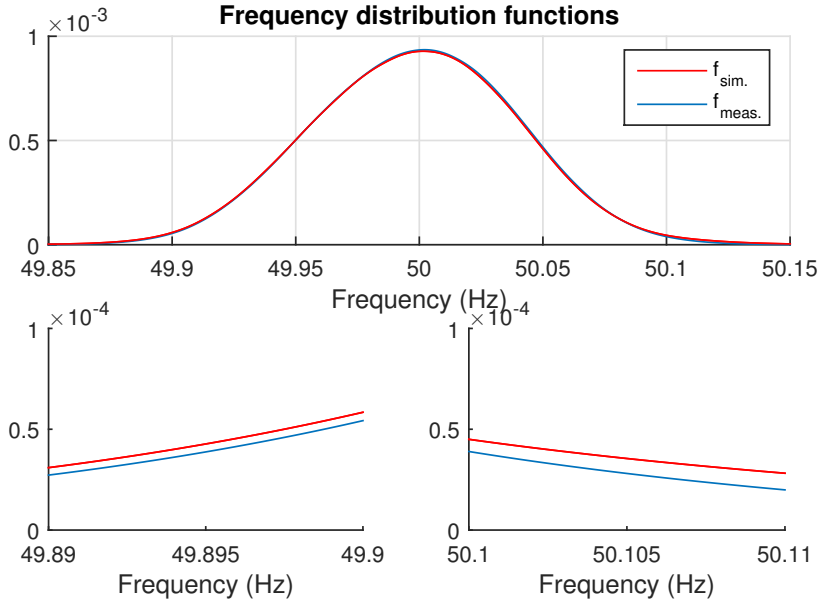

Figure 4.6: **Validation 3**. Frequency probability density functions for simulated and frequency measurements using data from 16-30 of July 2015.

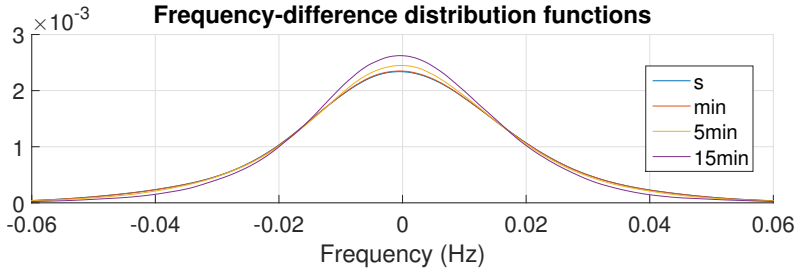

Figure 4.7: **Validation 4**. Frequency-differences probability density functions between average simulated frequency responses and average frequency measurements using data from 16-30 of July 2015.

Validation 3: This thesis evaluates the frequencies probability density functions. The probability density functions are the likelihood that a random sample would have the particular frequency value [55]. Figure 4.6 shows the high-resolution simulated model output using FABE and the historical high-resolution frequency measurement for 16-30 July 2015, using the identified system parameters from 1-15 of July.

Validation 4: This thesis also evaluates the frequency-differences' probability density functions. The frequency-differences' probability density functions indicate the likelihood of differences between simulated and the independent frequency measurements. Figure 4.7 shows the frequency-differences probability density functions for 16-30 July 2015, using identified system parameters from 1-15 of July.

4.4 Reference scenario

The references scenario, Base Case (BC), uses available multi-bidding zone data to re-create an imbalance time-series from a historical time-period described in Chapter 3. This thesis reproduces the strategies in the system-operational dispatch, for a particular time-period, using the RSG- and TFC-decisions at the same time. Method A has been used to identify the PFC reserve capacity (PFC^{cap}). Method B has been used to identify the division of PFC reserve capacities between bidding zones. However, grid code requirements have been used to divide the primary frequency control capacities between bidding zones for the bidding zones where the results of PFC reserve capacities were not satisfactory, i.e. SE1, SE2, SE3, SE4, DK2 and FI.

One of the overall conclusions of this thesis is that all these validations approach, i.e. Validation 1,2,3, and 4, indicate that the model (FABE) reproduces the normal state behaviours quite accurately. At least accurately enough to be used for research topics addressing issues regarding the normal state frequency and active power dynamics. The validated set-up: creating FABE in Chapter 3 and identified system parameters in Section 4.2.2; are from now on, in this thesis, used as a reference scenario called Base Case (BC). The identified system parameters, described in Section 4.2, were identified using data from 1 to 15 of July 2015. These parameters were validated using data from 15 to 30 of July 2015. In the next Chapter 5, this reference scenario is used to evaluate and compare new decisions for the time-period of July 2015.

Chapter 5

Modelling, testing and evaluating new decisions* with FABE

This chapter applies the balancing evaluation framework by testing different decisions impact on balancing operation. The chapter is based on [J1] and [C2]. Section 5.1 introduces this chapter. Section 5.2 identifies targets supporting the corporate missions of the System Operators (SOs). Section 5.3 models new decisions and the framework is applied on the Nordic Synchronous Area in Section 5.4. Finally, Section 5.5 concludes this Chapter.

* This thesis uses the term **decisions** for all the different actions that the SO can take before the actual operation moment in order to keep an efficient load-generation balance in the normal state.

5.1 Introduction

Chapter 3 presented an intra-hour model (FABE) using available multi-area data. Chapter 4 validated FABE on data for the Nordic Synchronous area from 16 to 30 of July 2015 using identified system parameters using data from the 1 to 15 of July 2015. Now, the verified model setup and identified system parameters are used as a reference scenario called Base Case (BC). For details and definition of BC, see Section 4.4.

This thesis compares the output using FABE to evaluate new decisions against BC. FABE creates various outputs such as frequency response, eACE, used automatic reserves among others. These outputs by themselves will not tell a SO how a tested new decision has performed. Instead, refining the output from the time-domain simulations, extends FABE-simulation results into targets supporting the missions of the SOs is needed. Section 5.2 identifies targets for the normal state operations that support the corporate missions of the SOs.

Section 5.3 models new decisions. There are many ideas for decisions that can and would have an impact on power system balancing operations. Reference [30, 56] presents many different SOs decisions improving power system operations. Decisions can be improving forecasts used in the operational dispatch, more proactive operational dispatch activations, changing the structure of the balancing market and increase flexible reserves among others. This thesis presents the following three modelled decisions published in [J1] and [C2].

Decision 1 (D1) is to lower the ramp rates for generation.

Decision 2 (D2) is to increase the automatic reserve capacities.

Decision 3 (D3) is a new strategy for the operational dispatch.

These new decisions are tested in Section 5.4 using data from July 2015. Results testing each decision are evaluated on their impact on selected targets supporting the SOs missions.

This Chapter finalises the Balancing Evaluation Framework (BEF) that finds more efficient decisions for transmission balancing operation.

5.2 Sub-Model 5: Processing metrics

Input: data is various time-series of the time-period (T) such as: $f_T^{sim.}$, $eACE_T^{sim.}$, $PFC_T^{sim.}$, $SFC_T^{sim.}$, $TFC_T^{sim.}$, and $RSG_T^{sim.}$.

Output: data are balancing metrics: frequency quality, average used reserve capacities and the Control Standard Performance 1 (CPS1) for the simulated time-period (T).

To find a *good decision*, one first needs to define what a good decision is. For a SO, a good decision is a decision supporting their missions. For example, ENTSO-E's mission is to work for [57];

(i) a secure and reliable power system;

(ii) a transparent market platform;

(iii) reducing-greenhouse-gas-emissions;

(iv) a sustainable network development.

This thesis compares new decisions impact on the normal state operational performance using selected balancing metrics as targets; supporting some of these missions.

The principal objective when selecting targets is to measure the performance in supporting the System Operators missions using the output from FABE. Many targets for measuring the System Operators performances exists [58]. However,

to operate the power system in a secure, reliable and economical manner is often essential when selecting these targets.

This thesis identifies the model output that can be selected as targets supporting ENTSO's missions. Also, the framework proposes to estimate an investment- and yearly costs for each decision to use it as an additional target (T4). In this thesis these cost estimations are roughly estimated and not outputs from the intra-hour model. Table 5.1 presents our interpretations of the missions of ENTSO-E.

Table 5.1: Selected targets supporting SOs missions

	Targets
T1	Time outside standard frequency range
T2	Used ancillary services
T3	Control Standard Performance 1 (CPS1)
T4	Costs, (investment and yearly)

Target 1 (T1) A secure and reliable power system (i); can regain a state of operating equilibrium after being subjected to a disturbance. Power system security can be referred to the degree of risk in its ability to survive imminent contingencies without interruption of customer service [5]. Hence, power system security depends on the system operating condition as well as the probability of dangerous contingencies. Reliability is the overall objective in power system operation. To be reliable, the power system must be secure most of the time [5]. The general industry practice has been the N-1 deterministic approach classifying the system operating condition [5]. The index *time outside the standard frequency range* indicates how often the system is in the normal security state and frequency stable even if the worst highly probable contingency would occur. Therefore a proposed target is *time outside the standard frequency range*. In the NSA the standard frequency range is 50 ± 0.1 Hz.

Target 2 (T2) A transparent market platform (ii); needs substantial liquidity of adjustable resources to be functional. By reducing allocated reserves for balancing, more resources are available for the daily markets. Hence, a proposed target is the used ancillary services. Here we calculate the used ancillary services by the used automatic reserve capacities (PFC, SFC) and the average activated system operational dispatch ($\langle P_{TFC} \rangle \& \langle P_{RSG} \rangle$).

Target 3 (T3) A sustainable network development (iv); is in need for SOs to use already existing networks more efficiently. Power systems are in Europe often divided into different bidding zones. By minimizing the need for reserved marginal over tie-lines for balancing power; existing tie-lines can be used more efficiently. Therefore,

a proposed target is the CPS1 metric used in the U.S. CPS1 is a combination of frequency and ACE [44]. To calculate CPS1, a frequency noise constant called a_{CPS1} is needed. The NSA has not an established value for the frequency noise constant. However, an estimated a_{CPS1}-value of -0.94 is used here. This value is only used here to compare different decisions impact on this target, i.e. the absolute value of this target is not valid within this study. Average 60 seconds values are used for these calculations [44],

$$CPS1^{sim.}_{n,60s} = 100 * (2 - a_{CPS1} * \frac{df}{dt}^{sim.}_{1,60s} * eACE^{sim.}_{n,60s}). \quad (5.1)$$

Target 4 (T4) Reaching these missions (i-iv) in a socio-economical form may be another goal. Roughly estimated costs for the investment and yearly costs for each decision can compute the total costs (5.2) by the investment costs added to four times the yearly costs. These roughly estimated total costs are proposed to be another target.

$$Cost^{tot.} = Cost^{inv.} + 4Cost^{year.} \quad (5.2)$$

5.3 Model new decisions in FABE

A purpose of this thesis is to illustrate how to use the balancing evaluation framework. To make this illustration this thesis develops and models new decisions. Three different decisions have been modelled.

Decision 1 (D1), is a grid code requirement, demanding lower ramp rates from fast regulated production.

Decision 2 (D2), is a grid code requirement, demanding an increased capacity of automatic reserves.

Decision 3 (D3), is a new strategy used in the system-operational dispatch. By forecasting a future frequency using data from a historical time-period, the SO can act more pro-actively.

Modelling decisions in FABE is performed for each new decision using the verified set-up except for the changes for the particular modelled decision.

5.3.1 D1: New ramp rates for generation

The decision is about decreasing the ramp rates for Fast Regulated Production (FRP). The decision has been modelled by changes in Sub-Model 1, described in Section 3.2. Each ramp started 10 minutes before (FRb) and ended 9 minutes after (FRa) each fast-regulated-production step-change instead of previously 5 minutes before and 4.5 minutes after.

Investment costs have been roughly estimated to be low. Balance Responsible Parties (BRPs) already distribute their FRP-ramps within the trading periods and

if the same procedure can be used but in a greater extent performing this decisions no investments are needed. Yearly costs have also been roughly estimated to be low.

5.3.2 D2: Increased automatic reserve capacities

This decision considers the possibility of increasing the normal state automatic reserve capacities. The decision has been modelled by changes in Sub-Model 3, described in Section 3.4. The primary-frequency-control capacity was increased by 100 $\frac{MW}{0.1Hz}$, from 620 $\frac{MW}{0.1Hz}$ to 720 $\frac{MW}{0.1Hz}$, i.e. by 16 percentages. The automatic reserves have been assumed to be delivered from the production however; it could be delivered from the demand in the future. Investment costs have been estimated to be low as a procurement process for primary-frequency-control reserves already exists. Yearly costs have been roughly estimated using a marginal cost of around 15 €/MW_{PFC}, in Denmark 2015 [59]. Marginal costs per hour times hours per year led to an estimated yearly cost of 13 M€/year.

5.3.3 D3: New proactive operational dispatch strategy

This decision aims to change the strategy used in the normal state operational dispatch by changes in Sub-Model 2, described in Section 3.3. This new proactive decision forecasts a frequency using available data in each time-step (t). This decision uses simulated frequency and scheduled production, consumption and HVDC-transmission that is already available in the system-operators control rooms today, i.e. no new information or data is needed. A forecasted frequency is used as a new control parameter in (3.19), described in Section 3.3, for decisions of TFC-activations. These activations will affect the system frequency when they are activated in AT-time from the present (t).

First, to obtain the forecasted frequency a new forecasted imbalance time-series (5.3) is calculated,

$$Y^{forc}_{2_{(K)}} = Y^{forc}_{1_{(K)}} + P^{D3}_{RSG_{(K)}}. \tag{5.3}$$

The new forecasted imbalance time-series (5.3) together with the frequency bias factor (B) are used with the real-time simulated frequency ($f^{sim}(t)$) to derive a forecasted frequency (5.4),

$$f^{forc}(t) = f^{sim}(t) - \frac{Y^{forc}_2(t) - Y^{forc}_2(t+AT)}{B}. \tag{5.4}$$

The new control parameter (5.5) uses the same TFC-confidence factor (K_{TFC}-=0.5) as in Section 3.3. However, instead of the simulated frequency a forecasted frequency (5.4) is used,

$$f_x(t) = f^{forc}(t). \tag{5.5}$$

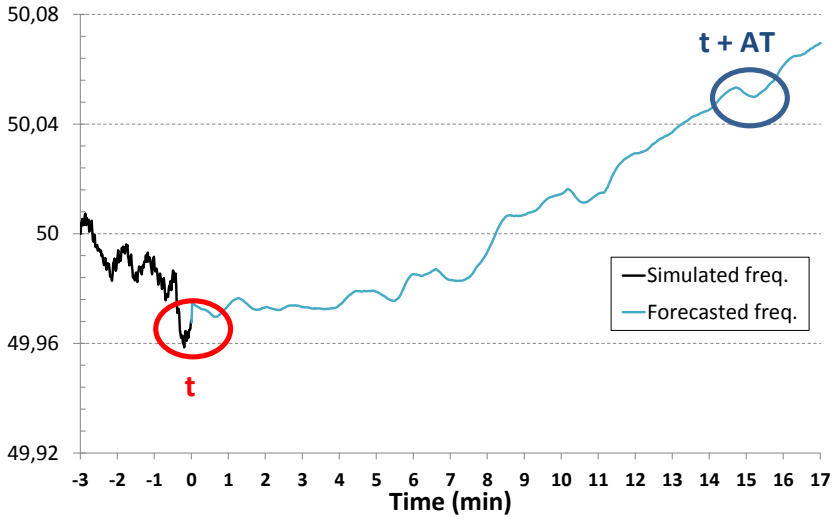

Figure 5.1: Illustration of the forecasted frequency AT from now (5.4), made at (t).

The implication of (5.5), illustrated in Figure 5.1, is that TFC-activation decisions are based on the present frequency and the forecasted frequency changes in TFC-activation time (AT) depending on present schedules and forecasts. This decision can be seen as a more proactive strategy for TFC-activations based on a forecasted frequency instead of the present frequency.

Investment costs for this decision have been estimated to be low if the tools helping the system operators performing this decision can be implemented in existing or new software that would have been built anyway. Also, yearly costs have been roughly estimated to be low as it is a change in the work-flow for the system-operational dispatch.

5.4 Test and evaluate new decisions using FABE

Finally, this thesis can complete the Balancing Evaluation Framework (BEF) by testing it on the Nordic Synchronous Area using bidding zone data from 1-30 of July 2015. Using the intra-hour model (FABE), created in Chapter 3; testing new decisions, developed in Section 5.3; refine each decisions simulation result to their impact on identified targets supporting corporate missions of the SOs, described

in Section 5.2; the decisions can be evaluated and compared against the validated reference scenario (BC), described in Section 4.4.

Results are illustrated in one figure and compiled in three tables. Figure 5.2 shows simulated frequencies as probability density functions. Results for Target 1 (T1) are compiled in Table 5.3; results for Target 2 (T2) in Table 5.4; results for Target 3 (T3) in Table 5.5; and for Target 4 (T4) in Table 5.2.

Table 5.2: Tested decisions & Target 4 (T4); roughly estimated costs (M€)

Case	Tested decisions	Costs		
		inv.	year.	tot.
BC	Reference scenario	0	0	0
D1	Lowering ramp rates from FRP by 2	0	0	0
D2	Increasing the normal state PFC-cap. by 100 $\frac{MW}{0.1Hz}$	0	13	52
D3	New TFC-decisions based on a forecasted frequency	0	0	0

Table 5.3: Target 1 (T1). Time outside standard frequency range (%). Tests performed on the time-period of 1-30 July 2015

Case	$f^{sim.} \prec 49.90$ (%)	$50.10 \prec f^{sim.}$ (%)	Total (%)
BC	0.37	0.54	0.91
D1	0.18	0.35	0.54
D2	0.11	0.2	0.31
D3	0.3	0.23	0.53

Table 5.4: Target 2 (T2). Average used ancillary services in (MW/hour). Tests performed on the time-period of 1-30 July 2015

Case	PFC	SFC	$\langle P_{TFC} \rangle$	$\langle P_{RSG} \rangle$	TOT
BC	620	0	221	19	860
D1	620	0	221	19	860
D2	720	0	221	19	960
D3	620	0	229	19	867

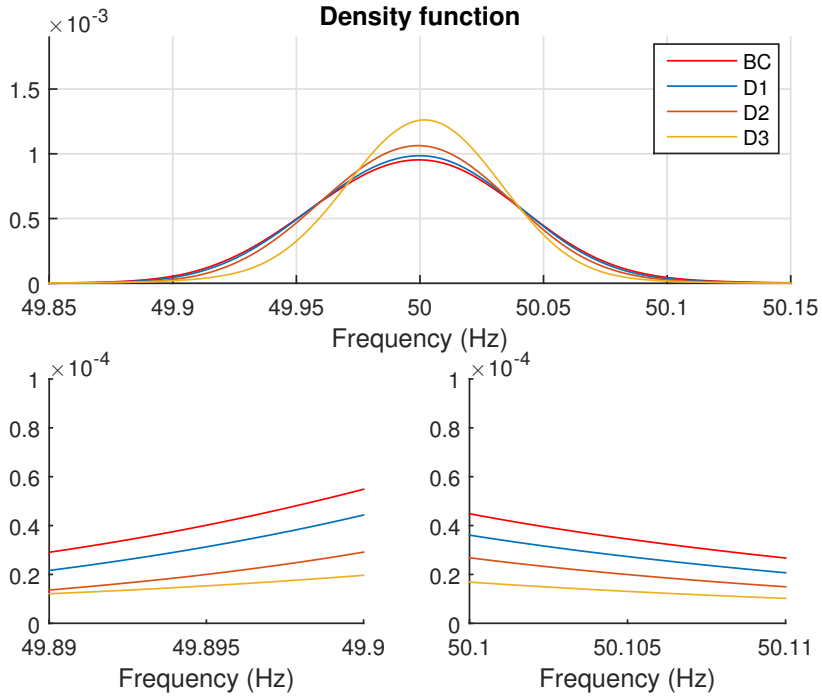

Figure 5.2: Target 1 (T1). Frequency density functions during the time-period of July 2015. The frequencies were divided into 0.0001 Hz wide bins and filtered with a zero-phase digital filtering [2] using 200 as filtering constant. The lower right and left panels are zoomed in using the upper panel.

D1: New ramp rates for generation

This case considers lower ramp rates for fast-regulated production by changing data-processing method K, described in Section 5.3.1. Results indicate the following:

(T1) Impact on Target 1, i.e. frequency quality, compiled in Table 5.3 and illustrated Figure 5.2, indicates that this decision can improve frequency quality significantly.

(T2) Impact on Target 2, compiled in Table 5.4, indicates that this decision has no impact on the need for reserve capacities.

(T3) Impact on Target 3 (Table 5.5) indicates that this decision has no effect on the CPS1 target compared to the reference (BC).

(T4) Impact on Target 4, the roughly estimated total costs (Table 5.3) indicates that total costs for implementing this decision compared to increasing PFC-capacities (D2) are estimated to be relatively low.

Table 5.5: Target 3 (T3). Control Performance Standard 1 (CPS1). Tests have been performed on the time-period of 1-30 July 2015. A good CPS1-performance for a bidding zone is 200.

	SE				NO					FI	DK
Case	1	2	3	4	1	2	3	4	5		2
BC	114	70	186	208	238	221	164	198	258	167	165
D1	116	71	186	210	239	220	167	200	259	175	169
D2	126	88	188	207	232	218	169	198	250	172	170
D3	172	172	181	191	189	196	213	209	190	163	183

	TOT	
Case	μ	σ
BC	181	49
D1	183	49
D2	183	43
D3	187	14

The impacts on Target 1, 2, 3 and 4, indicate that a SOs decision (lowering ramp rates of fast-regulated production) is as follows. Improved Target 1, i.e. frequency quality leads to improved system-operating conditions over time. Improved system operating conditions over time implies an improvement of the power system security and reliability [5]. The result that this decision (lowering ramp rates of fast-regulated production) improves T1 is in-line with [19] studying the impact of the decision on another power system.

To implement this decision, the SOs need to distribute starts and stops within the trading periods to a greater extent. Changing the balancing market structure and creating shorter trading period lengths may have a similar impact. The reason for this is that shorter trading period lengths may imply more distributed starts and stops within the trading periods of today.

D2: Increased flexible reserves (PFC-capacity)

This testing implies increasing primary-frequency-control capacities for all hours, modelled in Section 5.3.2. Results indicate the following:

(T1) Impact on Target 1, i.e. frequency quality, compiled in Table 5.3 and illustrated Figure 5.2, indicates that this decision can improve frequency quality significantly.

(T2) Impact on Target 2, compiled in Table 5.4, indicates that this decision is in a greater need of capacities for reserves, i.e. this decision has an negative impact on this Target 2.

(T3) Impact on Target 3 (Table 5.5) indicates that this decision improves T3 compared to the reference scenario BC. Results are closer to 200 average CPS1 value (μ) and the standard deviation between bidding zones (σ) are lower compared to BC.

(T4) Impact on Target 4, the roughly estimated total costs (Table 5.3), indicates that total costs may be relatively high compared to D1 and D3.

The impacts on Target 1, 2, 3 and 4, indicate that a SOs decision (increasing the PFC-capacity) is as follows. Improved Target 1, i.e. frequency quality leads to improved system-operating conditions over time. Improved system-operating conditions over time imply an improvement of the power system security and reliability [5]. Studying the impact of the decision on another power system [19] also reported that this decision improves T1. However, the impact on Target 2 indicates that this decision (increasing the PFC-capacity) is in need of more allocated resources for balancing operation. Allocating more resources for balancing operation will diminish the daily electricity markets liquidity. Moreover, the impact on the roughly estimated total costs indicates that this decision is more expensive than D1 and D3.

D3: New and more proactive operational dispatch

Testing new tertiary-frequency-control decisions based on a forecasted frequency has been modelled in Section 3.3. Results indicate the following:

(T1) Impact on Target 1, i.e. frequency quality, compiled in Table 5.3 and illustrated Figure 5.2, indicates that this decision can improve frequency quality significantly.

(T2) Impact on Target 2, compiled in Table 5.4, indicates that this decision has no impact on the need for reserve capacities.

(T3) Impact on Target 3 (Table 5.5) indicates that this decision improves T3 compared to the reference scenario BC. Results are closer to 200 average CPS1 value (μ) and the standard deviation between bidding zones (σ) are lower compared to BC.

(T4) Impact on Target 4, the roughly estimated total costs (Table 5.3), indicates that the roughly estimated total costs are low compared to an increased PFC-capacity (D2).

The impacts on Target 1, 2, 3 and 4, indicate that the SOs decision (new strategy for TFC-decisions) is as follows. Improved Target 1, i.e. frequency quality leads to improved system-operating conditions over time. Improved system-operating conditions over time imply an improvement of the power system security and reliability [5]. Improved Target 3, CPS1, indicates that this decision uses the already existing

transmission grid more efficient. This implication may not be correct as the modelled distribution of TFC-activations between bidding zones depend on the total planned production and not the location of the best-priced bid. The effect of this modelling error has to be studied more closely to use the CPS1 target evaluating this decision. Moreover, the impact on the roughly estimated total costs indicates that this decision may be more cost efficient than D1 and D2.

5.5 Discussion and Conclusions

Power systems are transformed to accommodate large volumes of vRES. Also, deregulation of electricity markets and increasing HVDC-transmission capacities between control areas have also transformed many power systems. All these changes have led to more imbalances for the SOs to handle. The SO can handle these imbalance control issues by many different decisions made at various stages before real-time operations.

This thesis introduces a new Balancing Evaluation Framework (BEF). The purpose of BEF is to evaluate many different decisions made at various stages before real-time. To test many different decisions, the framework creates an intra-hour model (FABE), able to capture the normal state frequency and active power dynamics. The framework evaluates new decisions using FABE on their impact on selected targets supporting corporate missions of the SOs.

The thesis tests the framework on a real power system called the Nordic Synchronous Area using data from 1-30 July 2015. To draw any overall conclusions of different decisions impact on balancing operation more data and time-periods are needed, however, from this test of modelling three new decisions have several implications.

The three tested decisions were: D1 - lower ramp rates for generation, D2 - increased PFC-reserve capacities, and D3 - a new operational-dispatch strategy. The implications of testing three different decisions made at various stages before real-time on selected targets supporting the SOs missions are as follows.

Target 1 Security and reliability. Impact on Target 1, i.e. frequency quality, illustrated in Table 5.3 and Figure 5.2, indicates that all three decisions improves frequency quality significantly. Improvement of Target 1 leads to improved system-operating conditions over time. Improved system-operating conditions over time imply an improvement of the power system security and reliability [5]. D2 - increasing PFC-reserve capacities with 16 percentages, enhances this target the most.

Target 2 Need for ancillary services. Impact on Target 2, compiled in Table 5.4, indicates that D1 and D3 are in no need for more ancillary services compared to D2 where more capacities for primary frequency control are used. Allocating more capacities for ancillary services will diminish the daily electricity markets liquidity.

Target 3 Control Performance Standard 1. A good CPS1 performance is close to 200. The impact on Target 3 (Table 5.5) indicates that D1 has no impact on T3 and D2 slightly improve T3 whereas D3 improves T3 significantly. D3 improves

Target 3 as the CPS1 value is closer to 200 as an average for all bidding zones (μ) and because the standard deviation between bidding zones (σ) are lower. Improved Target 3 (CPS1) indicates that these new decisions use the already existing transmission grid more efficient. However, the results of D3 improving Target 3 significantly may be due to improper modelling. The effect of this has to be studied more closely.

Target 4 Total costs. The roughly estimated total costs are just an illustration of how the framework can be performed. These results are not results of the rigorously work leading to the creation of the model FABE. However, these roughly estimated costs indicate that D1 and D3 seem to be more cost-efficient than D2. However, once again these are rough estimations of total costs that have been performed to exemplify how it can be done.

Overall implications of tests performed on July 2015. Finally, the thesis has now reached its primary goal by illustrating how one can apply the Balancing Evaluation Framework (BEF) on a real and large power system. To use BEF the thesis recommends that each SO identifies their own targets supporting their own goals and missions to find their decisions enhancing the normal state transmission balancing operation using the innovative intra-hour model (FABE) based on available multi-bidding zone data.

Chapter 6

Conclusions

This chapter presents concluding remarks in Section 6.1 and Section 6.2 presents major suggestions of future work.

6.1 Summary and concluding remarks

Power systems are transformed to accommodate large volumes of vRES. Also, deregulation of electricity markets and increased HVDC-transmission capacities between control areas transform many power systems today. All these transformations have led to more imbalances. These imbalances have to be controlled, and in liberalized power systems an organisation called System Operators has to handle them. This thesis addresses the problem in finding better decisions to control these imbalances.

First of all, the term imbalance can have several different meanings. Chapter 2 illustrates and defines the term imbalance used in this thesis. The definition of the term imbalance is the difference between real-time measurements and trades. It is divided into three components. The three components are variability, uncertainty and difference between forecasts and trades.

This thesis introduces a new Balancing Evaluation Framework (BEF) that can be used to find better decisions to control these imbalances. Many different decisions made at various stages before real-time can be evaluated. First, the framework creates an intra-hour model (FABE), able to capture the normal state frequency and active power dynamics. The framework evaluates new decisions using FABE on their impact on selected targets supporting corporate missions of the SOs.

Chapter 3 creates FABE. FABE simulates the operation second by second considering the different decisions, the load and production variation, the frequency, the system-operation dispatch and the automatic control in the studied system. One of the main motivations of developing FABE is that the structure of FABE makes it possible to test the impact from many different decisions on power system balancing operation.

Chapter 4 identifies system parameters using novel methods developed and tested in this thesis. The primary frequency control capacity is unknown in many power systems. In the normal state operation, the primary frequency control capacity is identified using two methods. The first method, based on simulated frequency and frequency measurements identifies the frequency control capacity and the frequency dependence of load for a particular time-period. It is tested, and results were satisfactory and in line with the general belief that the primary frequency control capacity increases during winter time.

Validating the identified system parameters and the intra-hour model (FABE) is performed in Chapter 4. Validation is a task demonstrating a model's reasonable representation of the actual system, i.e. the model should be able to reproduce system behaviours with enough fidelity to satisfy analysis objectives. Several different methods have been developed and tested to analyse the normal state active power and frequency dynamics. Results show that FABE can be trusted, representing the system behaviours with enough fidelity to satisfy its purpose.

The purpose and scope of this thesis have been to develop the framework (BEF) applicable to real and large power systems. Presented in Chapter 5, the framework is finalized by modelling, testing and evaluating three different decisions impact on selected targets supporting the corporate goals and missions of the SOs for the Nordic Synchronous Area during July 2015. The three different decisions were: D1 - lower ramp rates for generation, D2 - increased PFC-reserve capacities, and D3 - a new operational-dispatch strategy. To draw any overall conclusions of different decisions impact on balancing operation more data and time-periods are needed, however, from this test of modelling three new decisions have several implications. However, results indicate that all these three decisions can improve SOs selected targets significantly.

6.2 Future work

Major suggestions of future work are as follows:

* Network models could be used connecting all bidding zones high-resolution net-exchanges to perform power flow analyses.

  This thesis develops a multi-area model (FABE) without a connected network model. Instead, it considers each bidding zone for itself; estimating ACE using schedules and measurements from a historical time-period. Network models can be PTDFs or more detailed network models depending on analysed control issue. However, a recommendation is to develop new methods that can create network models using available historical data. These network models could be network models for a specific time-period of bidding zone structure that can be utilised performing power flow analyses on time periods for several months using high-resolution time-scales.

The implication of this improvement of connecting FABE to a network model would possibly be to evaluate different decisions performance on targets concerning power flows, such as the needed size of Transmission Reliability Margins (TRM) on tie-lines between bidding zones. Also, this could enhance the modelling of the system-operational dispatch making it possible to consider tie-line congestions.

* Find optimal decisions for transmission balancing operation.

  This thesis has developed a framework that can find more efficient decisions for the normal state transmission system balancing operation. However, the framework cannot find the optimal decisions for the normal state transmission system balancing operation. To find the optimal combination of decisions a method may be to transform many different decisions into variables. The sensitivity of an objective function considering selected targets supporting SOs missions to these decision variables could make it possible to find the overall optimal decisions.

  The implication of this improvement could be creating a balancing evaluation framework finding several optimal combinations of decisions depending on the SOs weights on the selected targets supporting their goals and missions.

* Apply the framework to future power-system scenarios.

  This thesis develops an intra-hour model validated against high-resolution normal-state measurements. One advantage using data from a historical time-period is that a validated reference scenario is obtained. Another advantage is that both schedules and measurements exist. Future power system scenarios can be used performing economic dispatches, i.e. physical electricity trading in future scenarios. However, to apply the framework on future scenarios, schedules and measurements for the future scenario are needed. New methods and approaches are required creating these future schedules and measurements.

  The implication of this improvement would make it possible to find more efficient and/or even the optimal decisions in future power systems. Applying the framework on future power system scenarios could generate a proactive balancing evaluation framework not only finding today's but also tomorrow's optimal balancing decisions.

* Many more decisions and time-periods could be tested using the framework.

  This thesis develops a framework that is applied on the Nordic Synchronous area for three different decisions on the time-period of July 2015. The three different decisions were: D1 - lower ramp rates for generation, D2 - increased PFC-reserve capacities, and D3 - a new operational-dispatch strategy. The framework could be used testing many more decisions such as other ramp

rates for generation and HVDC-transmission, other design and capacities of automatic reserves, changed trading period lengths, other system-operational-dispatch strategies, power system generation mix, improved forecasts of vRES and consumption, and different activation times of manual reserves among others.

The implication of using the framework to test many more decisions could help the System operators finding better decisions improving their goals and missions.

* Primary frequency control capacities for all bidding zones could be identified.

  This thesis develops a method that identifies the primary frequency control capacity based on simulated frequencies and frequency measurements. However, the primary frequency control capacity is also often unknown in many bidding zones. To address this issue the method could be improved including a network model together with tie-line schedules.

  An implication of this improvement of identifying the primary frequency control capacities in each bidding zone would be that it improves the intra-hour model FABE.

* The novel strategy using a forecasted frequency in the system operators control room could be tested.

  This thesis developed a new system-operational dispatch strategy. This strategy uses a forecasted frequency to control system-operational dispatch decisions. The strategy has been tested using the framework developed in this thesis on the Nordic Synchronous Area. Results indicate a very good performance using only already today existing control room data. However, this strategy could be further developed including tie-line constraints and how often the direction of dispatched reserves can be adjusted.

  The implication of implementing this strategy in the system-operation control rooms is indicated to improve selected targets supporting corporate missions of the SOs. This could improve the power system security and reliability in a cost effective way.

* More system variables could be included in the intra-hour model.

  The system security in any given moment depends on many different system variables. This thesis developed a new framework to evaluate many different decisions impact on balancing operation. Here, the framework uses the industry practice N-1 deterministic approach for frequency stability. However, power system frequency stability depends on many different system variables such as power system inertia, the automatic reserves speed and capacities

among others. More system variables could be included to improve the framework.

The implication of this improvement of including more system variables, such as power system inertia, would improve the framework and make it possible to select more targets supporting the corporate missions of the System Operators. It could also make it possible to test new types of decisions impact on the balancing operation. These new types of decisions could be increasing power system inertia and/or increasing the automatic reserves used for disturbances.

* New design of automatic reserves controlling the increasing imbalances could be tested.

  Most recently, due to the extensive accommodation of vRES, new types of reserves often called *Ramping Reserves* have been discussed to control highly unpredictable active power ramps from solar and wind causing large imbalances. The framework could be used to test new design and capacities of automatic reserves.

  The implication of this improvement of testing new types of automatic reserves could make it possible to find better and more optimal approaches to control the highly unpredictable active power ramps caused by solar and wind.

Bibliography

[1] Mathworks, *FFT for Spectral Analysis*, (2017, Apr 06) [Online]. Available: http://se.mathworks.com/.

[2] ——, *Zero-phase digital filtering*, (2016, Mar 17) [Online]. Available: http://se.mathworks.com/.

[3] I. E. Agency, "World energy outlook," 2015, [Online] Available: http://www.worldenergyoutlook.org/publications/weo-2015/.

[4] K. Gravett, "The electric light at godalming, 1881," *Surrey History, Vol.II No.3, Surrey Archaelogical Society, Guildford, 1981-82*, (2017, Aug 25) [Online]. Available: http://www.engineering-timelines.com.

[5] P. Kundur, J. Paserba, V. Ajjarapu, G. Andersson, A. Bose, C. Canizares, N. Hatziargyriou, D. Hill, A. Stankovic, C. Taylor, T. V. Cutsem, and V. Vittal, "Definition and classification of power system stability ieee/cigre joint task force on stability terms and definitions," *Power Systems, IEEE Transactions on*, vol. 19, no. 3, pp. 1387–1401, Aug 2004.

[6] L. Söder, H. Abildgaard, A. Estanqueiro, C. Hamon, H. Holttinen, E. Lannoye, E. Gómez-Lázaro, M. O'Malley, and U. Zimmermann, "Experience and challenges with short-term balancing in european systems with large share of wind power," *IEEE Transactions on Sustainable Energy*, vol. 3, no. 4, pp. 853–861, 2012.

[7] A. Molina-Garcia, I. Munoz-Benavente, A. Hansen, and E. Gomez-Lazaro, "Demand-side contribution to primary frequency control with wind farm auxiliary control," *Power Systems, IEEE Transactions on*, vol. 29, no. 5, pp. 2391–2399, Sept 2014.

[8] ENSTO-E, *European network of transmission system operators for electricity*, (2017, Oct 10) [Online]. Available: https://www.entsoe.eu/.

[9] "Proposal for a regulation of the european parliament and of the council on the internal market for electricity."

[10] R. G. W. J. Northcote-Green, *Control and Automation of Electrical Power Distribution Systems*, CRC Press, NW, US, Sep. 22, 2006.

[11] K. Morison, L. Wang, and P. Kundur, "Power system security assessment," *IEEE Power and Energy Magazine*, vol. 2, no. 5, pp. 30–39, Sept 2004.

[12] W. Wangdee and R. Billinton, "Bulk electric system well-being analysis using sequential monte carlo simulation," *IEEE Transactions on Power Systems*, vol. 21, no. 1, pp. 188–193, Feb 2006.

[13] L. Söder and L. B. Tjernberg, "Different time scales for studies of power system performance," in *North european power perspectives*, September 2011, pp. 1–2.

[14] *Frekvensreglering och lastfördelning på det svenska nätet*, Kungliga Vattenfallsstyrelsen driftbyrån, 1957.

[15] F. Falch Christensen, W. Wedeen, S. Mantinen, and H. H., "Time response for frequency-activated operating reserves in the nordel-network. recommendations based on system requirements and plant limitations," 1983.

[16] "Continuous ramping task force report," ENTSO-E, Brussels, Belgium, Jan. 2014.

[17] E. Moiseeva, M. R. Hesamzadeh, and D. R. Biggar, "Exercise of market power on ramp rate in wind-integrated power systems," *IEEE Transactions on Power Systems*, vol. 30, no. 3, pp. 1614–1623, 2015.

[18] "Frequency instability problems in north american interconnections," National Energy Technology Laboratory, Pittsburgh, PA, May. 2011.

[19] "Deterministic frequency deviations – root causes and proposals for potential solutions," ENTSO-E, Brussels, Belgium, Dec. 2011.

[20] *Energy roadmap 2050*, Tech. Rep., Brussels, Belgium, Dec. 2011.

[21] "Research evaluation of wind generation, solar generation, and storage impact on the california grid," KEMA, Inc, US., California, Jun. 2010.

[22] Y. Rebours, D. Kirschen, M. Trotignon, and S. Rossignol, "A survey of frequency and voltage control ancillary services mdash;part i: Technical features," *Power Systems, IEEE Transactions on*, vol. 22, no. 1, pp. 350–357, Feb 2007.

[23] "Analyses & review of requirements for automatic reserves in the nordic synchronous system," ENTSO-E, Brussels, Belgium, Jul. 2011.

[24] Y. G. Rebours, D. S. Kirschen, M. Trotignon, and S. Rossignol, "A survey of frequency and voltage control ancillary services;part ii: Economic features," *Power Systems, IEEE Transactions on*, vol. 22, no. 1, pp. 358–366, Feb 2007.

[25] "System needs and product strategy," 2017, [Online]. Available: https://www.nationalgrid.com/uk.

[26] J. Matevosyan, G. Thurnher, W. Katzenstein, and A. Stryker, "Ercot reserve adequacy study for the future system development scenarios with large share of renewable energy resources," in *2013 IEEE Grenoble PowerTech (POWERTECH)*, June 2013, pp. 1–6.

[27] J. Suh, D. H. Yoon, Y. S. Cho, and G. Jang, "Flexible frequency operation strategy of power system with high renewable penetration," *IEEE Transactions on Sustainable Energy*, vol. 8, no. 1, pp. 192–199, Jan 2017.

[28] E. Ela and M. O'Malley, "Studying the variability and uncertainty impacts of variable generation at multiple timescales," *IEEE Transactions on Power Systems*, vol. 27, no. 3, pp. 1324–1333, 2012.

[29] K.-O. Sandberg, *Kartläggning av frekvensreglering i det nordiska synkrona kraftsystemet - Ny strategi för balansregleringar från driftplaner?*, Teknisk-naturvetenskaplig fakultet UTH-enheten, Uppsala, Sweden, Juni, 2016.

[30] S. kraftnät, "Systemutvecklingsplan 2018-2017, oct 2017," *Systemutvecklingsplan 2018-2017*, (2017, Oct 22) [Online]. Available: http://www.svk.se/.

[31] NERC, "Procedures for validation of powerflow and dynamics cases," 2015, [Online]. Available: http://www.nerc.com.

[32] E. Allen, D. Kosterev, and P. Pourbeik, "Validation of power system models," in *Power and Energy Society General Meeting, 2010 IEEE*, July 2010, pp. 1–7.

[33] *Flexible Energy Scheduling Tool for Integrating Variable Generation (FESTIV)*, National Renewable Energy Laboratory, Colorado, USA. [Online]. Available: https://www.nrel.gov/.

[34] *KERMIT*, DNV-GL, Høvik, Norway. [Online]. Available: https://www.dnvgl.com/.

[35] *Electric System Intra-Hour Operation Simulator (ESIOS)*, Pacific Northwest National Laboratory, Richland, USA. [Online]. Available: https://www.pnnl.gov/.

[36] E. Ela, M. Milligan, and M. O'Malley, "A flexible power system operations simulation model for assessing wind integration," in *2011 IEEE Power and Energy Society General Meeting*, July 2011, pp. 1–8.

[37] L. S, P. Etingov, D. Meng, C. J. X Guo, and N. Samaan, "Nv energy large-scale photovoltaic integration study: Intra-hour dispatch and agc simulation," 2013, [Online]. Available: http://www.pnnl.gov/.

[38] H. Bevrani, *Robust Power System Frequency Control*, University of Kurdistan, Sanandaj, Iran, 2009.

[39] C. Hamon, *Probabilistic security management for power system operations with large amounts of wind power*, Universitetsservice US AB, Stockholm, Sweden, May. 29, 2015.

[40] *Historical measurements*, Nord Pool AS, Lysaker, Norway. [Online]. Available: http://www.nordpoolspot.com/.

[41] *Historical schedules and forecast data*, Svenska kraftnät (Swedish national grid), Stockholm, Sweden. [Online]. Available: http://www.svk.se/.

[42] Mathworks, "Piecewise cubic hermite interpolating polynomial (pchip)," 2015, [Online] Available: http://se.mathworks.com/.

[43] *Continental Europe Operation Handbook*, ENTSO-E, Brussels, Belgium, Jun. 2004.

[44] "Balancing and frequency control," NERC, Princeton, NJ, Jan. 2011.

[45] N. R. E. Laboratory, "Operating reserves and variable generation," 2011, [Online]. Available: http://www.researchgate.net/.

[46] P. Kundur, *Power System Stability and Control*, McGraw-Hill Inc., NY, 1994.

[47] H. Saadat, *Power System Analysis*, 3d ed., PSA Publishing LLC, US, 2010.

[48] J. Brownlee, "Overfitting and underfitting with machine learning algorithms," 2016-03-21, [Online]. https://machinelearningmastery.com/.

[49] NERC, "Compliance application notice — 0040," 2015, [Online]. Available: http://www.nerc.com.

[50] A. Ritter, "Deterministic sizing of the frequency bias factor of secondary control," 2015, [Online]. Available: www.eeh.ee.ethz.ch.

[51] ENTSO-E, "Agreement (translation) regarding operation of the interconnected nordic power system (system operation agreement)," 2006, [Online]. Available: https://www.entsoe.eu.

[52] J. Hillston, "14 model validation and verification," *The University of Edinburgh*, (2017, Oct 21) [Online]. Available: https://www.ed.ac.uk.

[53] "Power system model validation," North American Electric Reliability Corporation (NERC) 2015, [Online]. Available: http://www.nerc.com.

[54] P. Stoica and R. Moses, "Spectral analysis of signals," 2004, [Online]. Available: http://user.it.uu.se/.

[55] A. N. Kolmogorov, *Foundations of the Theory of Probability*, 2nd ed. Chelsea Pub Co, Jun. 1960. [Online]. Available: http://www.clrc.rhul.ac.uk/resources/fop/Theory...

[56] *Challenges and Opportunities for the Nordic Power System*, Svenska kraftnät, Stockholm, Sweden, Aug. 2016.

[57] "Entso-e's missions," European Network of Transmission System Operators for Electricity, 2016-03-18, [Online] Available: https://www.entsoe.eu/.

[58] "Performance measurements of generation and transmission systems," *Public Utilities Commission of Sri Lanka*, (2017, Nov 15) [Online]. Available: http://www.pucsl.gov.lk/.

[59] *FCR, Frequency Containment Reserves, DK2 Data*, Energinet.dk (Danish national grid), Fredericia, Denmark. [Online]. Available: https://en.energinet.dk/Electricity/Energy-data.